Wiley Online Library
Early View publication on www.wileyonlinelibrary.com
(issue and page numbers not yet assigned;
citable using Digital Object Identifier – **DOI**)

Laser Photonics Rev., 1600116 (2017) / **DOI** 10.1002/lpor.201600116

LASER & PHOTONICS REVIEWS

Abstract In the development of microfluidic chips, conventional 2D processing technologies contribute to the manufacturing of basic microchannel networks. Nevertheless, in the pursuit of versatile microfluidic chips, flexible integration of multifunctional components within a tiny chip is still challenging because a chip containing micro-channels is a non-flat substrate. Recently, on-chip laser processing (OCLP) technology has emerged as an appealing alternative to achieve chip functionalization through in situ fabrication of 3D microstructures. Here, the recent development of OCLP-enabled multifunctional microfluidic chips, including several accessible photochemical/photophysical schemes, and photosensitive materials permiting OCLP, is reviewed. To demonstrate the capability of OCLP technology, a series of typical microcomponents fabricated using OCLP are introduced. The prospects and current challenges of this field are discussed.

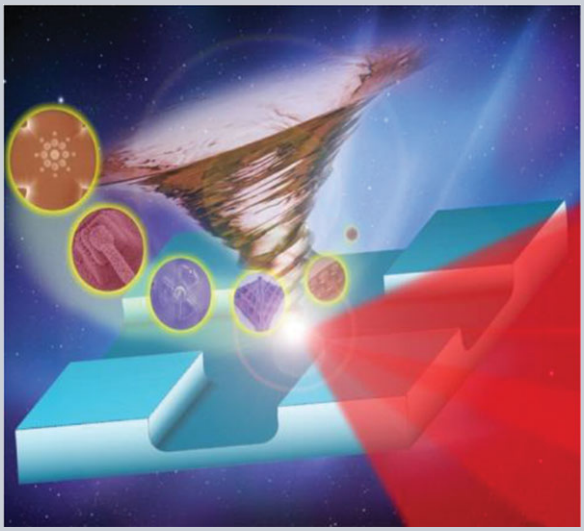

REVIEW ARTICLE

On-chip laser processing for the development of multifunctional microfluidic chips

Huan Wang[1], Yong-Lai Zhang[1,*], Wei Wang[1], Hong Ding[2], and Hong-Bo Sun[1,3,*]

1. Introduction

As a type of portable, eco-friendly, safe and highly efficient experimental platform, multifunctional microfluidic chips, also referred to as lab-on-a-chip systems, have attracted enormous research interest in recent decades due to their promise in both fundamental science and practical applications, ranging from chemical experiments [1–3], environmental monitoring [4, 5], biological assays [6–14], and tissue engineering [15–19] to medical diagnosis [20–23] and therapeutics [24–27]. Currently, by integrating various micro-scale components on a microfluidic chip, multiform experimental procedures, such as temperature regulation [28], nanoparticle synthesis [29–31], molecular detection [32], and cell manipulation [33–39], can be implemented in a controlled fashion. From a technical point of view, the rapid progress in microfluidic chip technology is driven by the constant advances in nanotechnology. As a typical example, well-developed semiconductor processing techniques enable the facile manufacturing of various microfluidic chips. Complex microfluidic channels with different sizes and designable shapes can be readily fabricated in a wide range of materials through the combined technologies of lithography and etching [39–42]. To pursue greater resolution or a controllable height-width ratio, deep reactive-ion etching (DRIE) [43], inductively coupled plasmas (ICP) [44] and other advanced processing techniques have also been used to fabricate microfluidic chips. Recently, to further enhance production efficiency, imprinting [45–47] and soft lithography [48–50] technologies have been successfully adopted to manufacture polymer microfluidic chips by duplicating hard templates machined using traditional methods.

Despite pronounced success in manufacturing microfluidic chips, the progress in multifunctionality remains restricted by the lack of technology that permits the flexible integration of various functional components; this significantly limits broad application. First, microfluidic chip manufacturing is generally based on conventional planar processes, such as lithography and imprinting. However, the integration of functional components requires precise fabrication of microstructures within microfluidic channels, which are not flat. In addition, traditional methods can process only two-dimensional (2D) microstructures; the integration of three dimensional (3D) functional micronanostructures within microfluidic chips is still challenging [51].

[1] State Key Laboratory on Integrated Optoelectronics, College of Electronic Science and Engineering, Jilin University, 2699 Qianjin Street, Changchun, 130012, P. R. China
[2] State Key Laboratory of Inorganic Synthesis and Preparative Chemistry, College of Chemistry, Jilin University, 2699 Qianjin Street, Changchun, 130012, P. R. China
[3] College of Physics, Jilin University, 119 Jiefang Road, Changchun, 130023, P. R. China
*Corresponding authors: e-mail: yonglaizhang@jlu.edu.cn; hbsun@jlu.edu.cn

Moreover, materials suitable for processing are limited to polymers, glass or silicon, which cannot meet the demands of multiform functional materials [52]. All of these obstacles have become bottlenecks restricting progress in the exploration, development and application of multifunctional microfluidic chips.

In recent years, laser processing technologies have emerged as an appealing alternative to conventional semiconductor processing techniques, making it possible to integrate various functional devices into microfluidic chips [53]. To achieve on-chip laser processing (OCLP), several photochemical and photophysical schemes, including laser ablation as a subtraction-type process [54, 55], and photopolymerization [56–58], photoreduction of metal ions [59] and photodynamic assembly of nanoparticles [60, 61] as addition-type processes, have been successfully developed for on-chip structuring of various functional materials such as glass, polymers [62–64], metals [65], biomaterials [66, 67] and nanomaterials [68]. Compared with traditional micronanofabrication technologies, OCLP has the distinct advantages of high precision, the ability to use multiform processing-capable materials, and site-specific fabrication. Specifically, when an ultra-short-pulse laser has been adopted for on-chip processing, thermal effects can be significantly suppressed, and thus the spatial resolution can be further improved [69]. As a typical example, femtosecond laser on-chip processing enables 3D fabrication with sub-50 nm precision at any desired position [70], and thus has substantial potential in the development of multifunctional microfluidic chips.

In this review, we summarize the recent advances of OCLP for microfluidic chip functionalization. First, we introduce the fundamentals of laser processing, including various photochemical/photophysical schemes. We then comprehensively review multiform photosensitive materials that allow for OCLP and several representative multifunctional microfluidic chips fabricated using OCLP. Finally, a brief conclusion and future prospects are presented based on our opinions.

2. Photochemical and photophysical schemes for OCLP

In the development of multifunctional microfluidic chips, advanced micronanofabrication technologies play a critical role. At present, classical "top-down" and "bottom-up" approaches, such as lithography, soft lithography, 3D-printing and self-assembly have been successfully used for both the manufacturing and functionalization of microfluidic chips. Among these techniques, laser processing is distinguished due to its key capability of integrating multifunctional micronanostructures within general microfluidic chips. To date, OCLP has been applied to various materials using different processing mechanisms. In this section, we briefly summarize several currently available photochemical/photophysical schemes that enable OCLP.

2.1. Laser ablation

As a subtraction-type processing mechanism, laser ablation can micromachine target materials into geometrically complex 2D/3D structures [54, 71–77], making it possible to prepare functional components on a microfluidic chip. Typically, when a pulse is applied to a target, electrons are excited from the ground state, followed by electron-electron scattering, electron-lattice scattering and other relaxation interactions [69]. During this period, the excited electrons heat the lattice, which can melt or evaporate the target if the temperature is high enough. The heating effect, together with shockwave emission, re-solidification and other affiliated effects, leads to the formation of permanent damage on the target and achieves the desired processing. Depending on the width of the laser pulses, laser ablation can be classified into long-pulse laser ablation and ultra-short-pulse laser ablation. Long-pulse ablation primarily excites electrons through linear absorption. Conversely, ultra-short-pulse ablation excites metal material electrons also through linear absorption [78], whereas electrons in semiconductor and dielectric materials are excited in a non-linear absorption manner [79].

When long-pulse lasers that have pulse durations significantly longer than the electron-lattice scattering time are employed in the processing, excited electrons transfer laser energy to the lattice before the pulse has terminated. The laser simply "heats" the solid, and the damage has been done at a relative large heat-affected zone due to thermal diffusion, (Fig. 1a) [80]. Conversely, if an ultra-short-pulse has been used, thermal effects could be effectively suppressed (Fig. 1b) [80]. Since the pulse duration is much shorter than the electron-lattice scattering time, laser energy associated with the pulse can be deposited into the electrons before they are transferred to the lattice. Thus, the material in the laser interaction region is ejected in the form of hot dense plasma. To clarify further, the timescale of an ultrashort pulse laser ablating transparent targets is shown in Fig. 1c, from which a conclusion can be reached that there is not enough time for the heat to diffuse during ultrafast laser ablation [69]. In general, the zone that is affected by ultra-short pulse laser is only a small area of focus, whereas a long-pulse laser induced heat-affected zone is much larger. In this regard, the resolution can be greatly improved through the use of an ultra-short-pulse laser [78], and hence ultra-short-pulse lasers are preferred in the fabrication of microfluidic chips [51].

Taking advantage of the improved 3D processing capability, ultrafast laser ablation shows great potential for a designed fabrication of the 3D microfluidic chips based on glass or polymers [54, 70]. Notably, 3D chips are promising for the future of microfluidics, because they can make full use of the vertical volume, above and below the microchannels, to improve the space utilization of the chip. Moreover, 3D chips have distinct advantages such as high throughput, low contamination, high efficiency, and the enabling of a 3D laminar flow for novel functionalities, such as 3D hydrodynamic focusing [81]. However, for

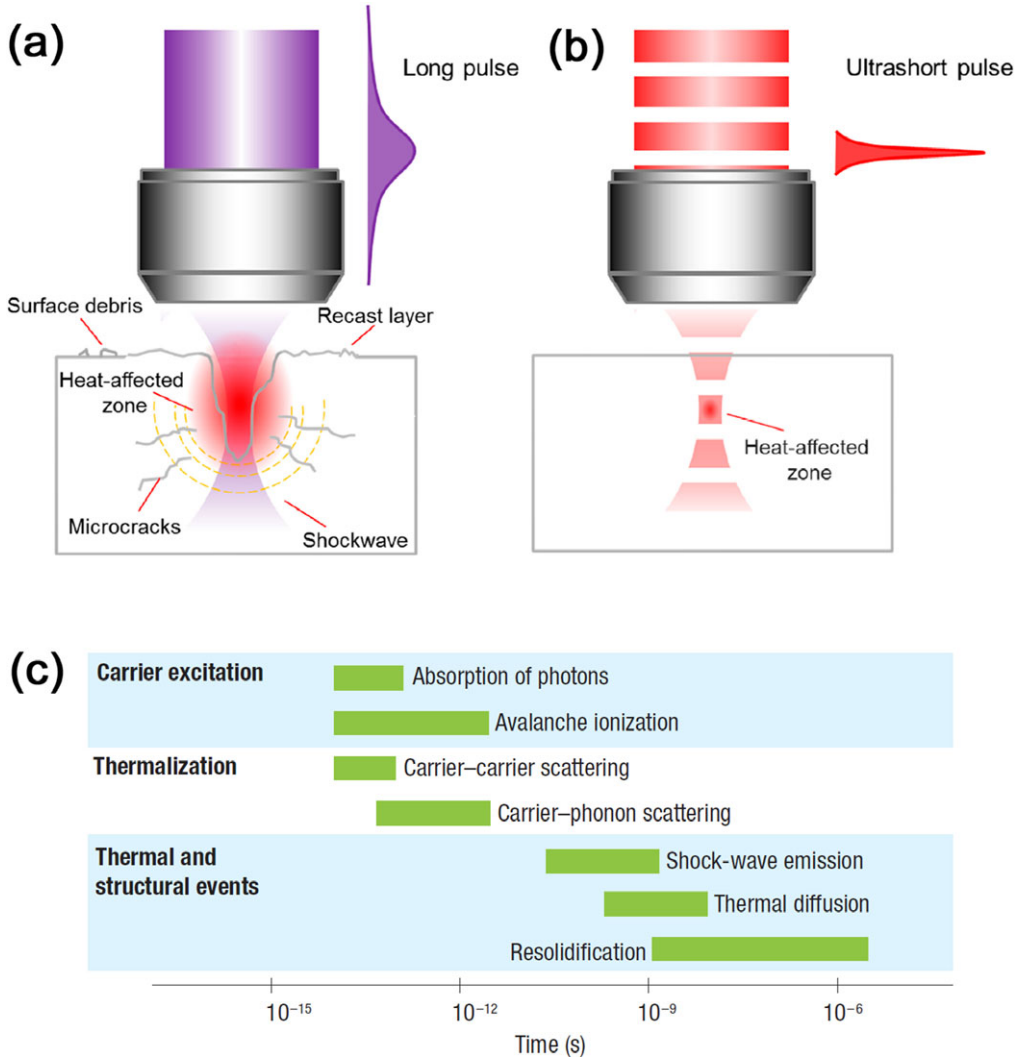

Figure 1 (a, b) Interaction between transparent targets and long/ultrashort pulse lasers. Heat-affected zone of long pulse laser ablation is much larger than that of ultrashort pulse ablation. (Reproduced with permission. [80] Copyright 2014, Multidisciplinary Digital Publishing Institute) (c) Timescale during interaction of ultrashort laser pulses with transparent materials. (Reproduced with permission. [69] Copyright 2008, Nature Publishing Group)

conventional 2D lithographic technologies, it is almost impossible to fabricate 3D microchannel networks, excluding the precise assembly of the PDMS layers [82]. In this regard, OCLP holds great promise for the development of the 3D microfluidic chips.

2.2. Laser induced photo-polymerization

Laser induced photo-polymerization is another widely used photochemical strategy that enables 3D fabrication with a high spatial resolution [83–86]. Generally, photopolymers consist of monomers or pre-polymers, cross-linkers, photo-initiators and photosensitizers among which monomers or pre-polymers and cross-linkers form the main networks; the photo-initiators and photosensitizers are added to improve the energy transferring routes [87]. Taking radical polymerization as an example, after absorbing sufficient photons, photosensitizers can transfer energy to the photo-initiators, and the excited photo-initiators can break the unsaturated bonds in the monomers forming radical monomers and triggering photo-polymerization [88]. In addition to radical polymerization, ionic polymerization, primarily based on ring opening and crosslinking of the oxirane groups, also enables laser fabrication [58]. However, ionic polymerization is less popular in the field of laser induced photo-polymerization because additional heat treatment is generally necessary to improve the polymerization.

For photo-polymerization, the absorbed photon energy should be large enough to trigger polymerization reactions. In the case of a UV laser, photons with high energy excite monomers to polymerize from the surface toward the inner parts, and the photo-polymerization is typically based on a single photon absorption (SPA) process. For long

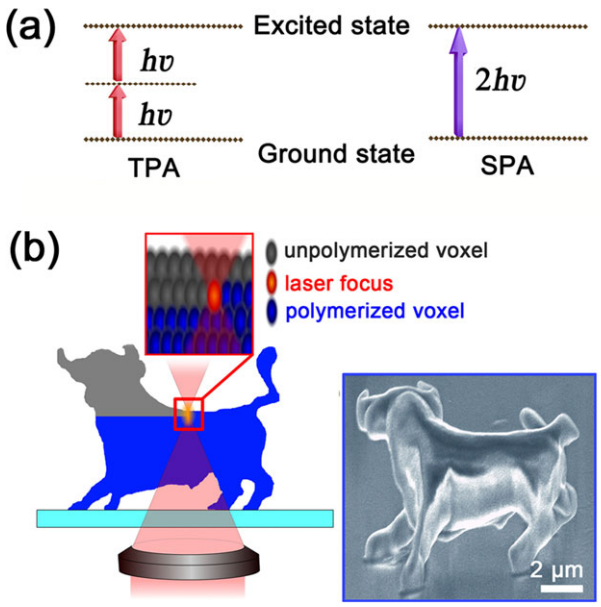

Figure 2 (a) Principles of TPA and SPA. When the density of photons is high enough, electrons of ground state could be excited by simultaneously absorbing two photons, which is called TPA. While photons with enough energy could directly excite electrons of gound state by aborbing only one photons. (b) A 3D nanobull fabricated by femtosecond laser induce photopolymerization. (Reproduced with permission.[83] Copyright 2001, Nature Publishing Group)

wavelength lasers, such as a femtosecond laser with an 800 nm wavelength, a single photon does not have sufficient energy, and monomers can absorb two or more photons in a small absorption cross-section, as shown in Fig. 2a. This phenomenon is known as two-photon absorption (TPA) or multi-photon absorption (MPA) [83, 87, 89].

Because TPA- or MPA-induced photo-polymerization occurs only within a small volume in the center of the laser focus, 3D micronanostructures with high spatial resolution beyond the optical diffraction limit can be readily fabricated (Fig. 2b). Taking advantage of the "direct writing" feature, TPA/MPA-induced polymerization is not restricted by the nonplanar surfaces of microfluidic chips and is thus an important method of integrating multifunctional micronanostructures within given microfluidic chips [51, 90, 91].

As an addition-type processing technique, TPA/MPA-induced polymerization enables integration of the 3D functional structures within a given microfluidic channel, revealing great potential for chip functionalization [92, 93].

Recently, numerous papers have reported the importance of the 3D cell-culture matrices for a controllable differentiation of stem cells [94, 95]. From this standpoint, integration of microstructures that mimic *in-vivo* environment would directly contribute to the tissue engineering field, and the applications of microfluidics would extend to the organ-on-chip, and even body-on-chip systems [94]. However, current limitations of the photo-polymerization induced chip functionalization lie in the use of commercial photoresists. In fact, materials with high biocompatibility are highly desirable for bio-chip applications. Fortunately, with the rapid progress of MPA technology, various hydrogels and proteins can now be processed by laser [96–98]. In addition, doping with other functional materials would further broaden the applications of photo-polymerization in chip functionalization [99].

2.3. Laser induced photoreduction

To further develop more processable materials, laser-induced photoreduction has been adopted for the fabrication of metallic micronanostructures [100–102]. Optical energy has long been used for photoreduction reactions, as evidenced by film photography. Among optical sources, lasers with a high energy density and monochromaticity are undoubtedly preferred [90, 103]. Taking Ag^+ as an example; under laser radiation, Ag^+ might be excited to an active intermediate state that could capture electrons from the surroundings and finally be reduced to Ag using an SPA or MPA process [104]. Typically, femtosecond laser-induced photoreduction of Ag^+ has been used to fabricate many multifunctional microfluidic chips [51]. A general mechanism is illustrated by the following formulas, which describe the photoreduction course of Ag^+.

$$Ag^+ + 2\,h\nu \longrightarrow Ag^{+}*$$

$$2Ag^{+}* + HO-\underset{\displaystyle CH_2-COO^-}{\overset{\displaystyle CH_2-COO^-}{\overset{|}{\underset{|}{C}}}}-COO^- + OH^- \longrightarrow 2Ag + CO_2 + H_2O + O=\underset{\displaystyle CH_2-COO^-}{\overset{\displaystyle CH_2-COO^-}{\overset{|}{\underset{|}{C}}}}$$

Although Ag^+ can be reduced to Ag under laser irradiation, it is still challenging to control the as-formed micronanostructures. For example, Ishikawa *et al.* tightly focused a femtosecond laser at the interface between a $AgNO_3$ aqueous solution and a cover slip to induce the growth of Ag structures [105]. They found that when a larger laser power and a greater exposure time were used, more Ag^+ was reduced to Ag sediment. Nevertheless, the morphologies of the Ag structures were irregular and were independent of the laser power and exposure time. Cao *et al.* found that the growth of Ag nanoparticles (NPs) was uncontrollable. Therefore, an entire Ag structure fabricated in this manner

typically has a poor morphology [106, 107]. In this regard, producing small and uniform Ag NPs was essential to obtain refined Ag structures. To achieve this end, surfactants that are widely used for controlling the shape and size of NPs were added to the precursor solution, and the morphology of the resultant Ag structures were significantly improved [59]. By using proper surfactants and concentrations, even 3D Ag microstructures [106] were successfully achieved.

In addition, the as-formed Ag NPs have a strong surface plasmon resonance (SPR) effect that can significantly influence their further growth; this has been confirmed by many teams [108–110]. Generally, SPR is induced in the direction of laser polarization, and many electrons gather at the poles of the dipoles with high photochemical activity where more Ag^+ can be reduced. Pre-produced Ag NPs can store electrons and deliver them to active Ag^+ to enhance the photochemical reactions. As a consequence, nanoplates are obtained due to the non-symmetrical growth, and the orientation is coincident with the laser beam polarization. Additionally, electrostatic forces, gradient forces, heat effects and other factors also influence the reduction and assembly of Ag NPs [111]. All of these effects should be taken into account when processing metallic microstructures.

2.4. Laser induced photodynamic assembly

Since Ashkin at Bell Telephone Laboratories first found that a beam could exert a force on tiny particles in 1969, increasing attention has been given to the remote, non-contact, non-destructive, controllable optical manipulation of micro/nanospecies. Optical trapping (OT) has been widely used to assemble colloidal particles [61, 112]. Different mechanisms are used to explain the phenomena when trapping particles are of a geometric optical size ($r>>\lambda$, where r is the radius of particle and λ is the wavelength of the light) or Rayleigh size ($r<<\lambda$). Geometric optical particles change the direction of the beam that propagates through the particles. Based on the momentum conservation law, the particles would have a gradient force exerted on them in the direction of the laser focus [113, 114] in a manner similar to a sphere being caught by the focus (Fig. 3a). In contrast, the OT of Rayleigh particles can be explained by an electromagnetic model [115]. Since the beam is an electromagnetic wave in essence, and Rayleigh particles can be polarized to become dipoles, the charged particles can be attracted to the electromagnetic potential wells of the beam where they would have the lowest energy [116–118], as shown in Fig. 3b. Because the exerted forces, also called gradient forces, are induced by the non-uniform optical fields, controlling the distributions of optical fields directly enables the photodynamic assembly of various functional colloidal particles.

Traditional OT has been adopted to manipulate NPs [61, 119], cells [120], and proteins [121], however, in the case of a laser-induced photodynamic assembly, it is inefficient when only using one beam. Recently, a spatial

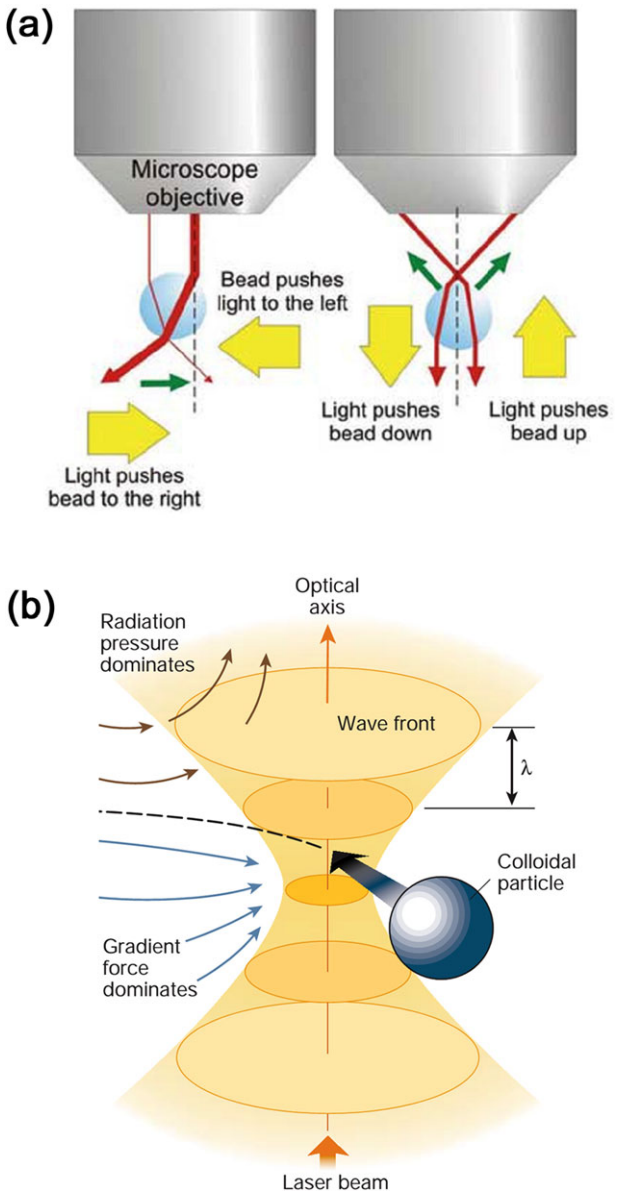

Figure 3 The principles of optical trapping. (a) Trapping NPs in geometric optical size is illustrated by geometrical optics. (Reproduced with permission.[113] Copyright 2006, Elsevier) (b) Trapping NPs in Rayleigh size is expained by electromagnetic theory. (Reproduced with permission.[116] Copyright 2003, Nature Publishing Group)

light modulator (SLM) [122] and near-field optical devices [123–126] have been introduced to produce non-uniform distributions of optical fields in a specific area, greatly improving the efficiency of the processing. To enhance the intensity gradient of optical fields, metal micro/nanostructures have been fabricated to increase the gradient forces generated using SPR [127–129], which could further suppress Brownian motion that disturbs the controllable assembly of NPs. Moreover, the high resolution of metal nanostructures can enable accurate assembly beyond the optical diffraction limit [130]. With the help of

OT, many useful devices consisting of colloidal particle assemblies can be integrated within microfluidic chips using a laser induced photodynamic assembly process.

3. Materials for the OCLP

According to principles outlined above, various photosensitive materials have been successfully used for both the fabrication and functionalization of microfluidic chips. Typically, when developing multifunctional microfluidic chips, glass, polydimethylsiloxane (PDMS), and photoresists are first machined using OCLP. Then, functional devices that consist of metal, polymer composites, nanoparticles or proteins are integrated within the given microfluidic chips using OCLP. In this section, a series of important photosensitive materials that permit OCLP are reviewed from the viewpoint of materials.

3.1. Glass

As cheap, stable and biocompatible materials, photosensitive glass is quite suitable for manufacturing multifunctional microfluidic chips using laser processing [55]. Because they are transparent to a non-resonant femtosecond laser, 3D microfluidic channel networks and even functional microstructures could be directly integrated within a bulk glass chip, suggesting substantial potential for the development of multifunctional microfluidic chips [131–134]. Commercial Foturan glass, which is made of lithium aluminosilicate and doped with Ag and Ce ions, is a widely used photosensitive material that allows laser processing [135, 136]. When excited by ultraviolet irradiation, Ag^{+} can capture the electrons released from Ce^{3+} ions, forming Ag clusters that act as crystal nuclei and promote the crystallization of lithium metasilicate. Because HF can etch the crystallized region faster, the irradiation areas can be selectively etched away, leaving cavities and channels in the bulk glass.

Fused silica is another kind of glass that permits laser processing, although the process is different with Foturan glass. As a typical example, a femtosecond laser could be used to fabricate nanogratings inside bulk-fused silica [137, 138]. Because the modified regions can be etched faster than other regions, microchannels can be fabricated using a combined process of direct laser writing and subsequent etching in HF or KOH solutions under ultrasonic cleaning [138–145]. In the case of fused silica, postannealing is generally required to obtain smooth surfaces. However, it is worth pointing out that the as-prepared microfluidic channels are not uniform. The channels near the outlet might be etched much more than the inner channels [146]. To address this problem, Liao *et al.* used porous glass with 10 nm nanopores immersed in water to fabricate uniform microchannels through femtosecond laser direct writing [70, 147, 148]. As illustrated in Fig. 4, water was introduced to the processing system to carry the scraps out

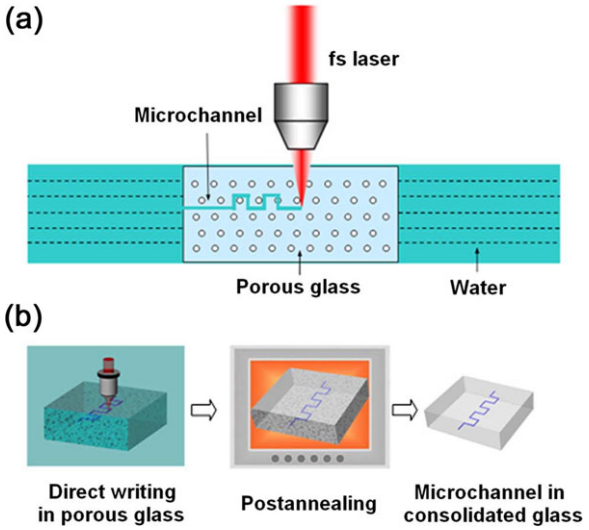

Figure 4 (a) Schematic illustration of laser microfabrication processing inside porous glass. (b) The fabrication procedure of a microchannel in porous glass. Postannealing is needed to eliminate nanoholes and obtain smooth surface of microchannels. (Reproduced with permission.[147] Copyright 2010, Optical Society of America)

of the channels or into the pores of the porous glass. In this manner, the generated scraps did not block the channels that had been machined. After laser microfabrication, postannealing treatment was applied to consolidate the glass matrix and eliminate the nanopores. Without being selectively modified and wet etched, the sizes and morphologies of the cavities are influenced only by the laser scanning tracks; therefore, both the shapes and sizes of the channel are controllable. Notably, complex 3D microfluidic channels with designable networks could be machined in this way, allowing more sophisticated biochemical reactions.

3.2. Polymers

Heat and light-cured polymers are two typical soft materials that are widely used for the fabrication of microfluidic chips. As a representative material, PDMS is well known for its flexible shaping and ideal optical characteristics. However, in most cases, PDMS is solidified using a heat-curing process. OCLP only helps to perform some modification processes [149–151]. For example, Huft *et al.* applied multilayer soft lithography (MSL) to assemble 3D multilayer PDMS channels whose interconnections between adjacent or separated layers were broken using laser microfabrication [82]. Currently, PDMS can be cured using femtosecond laser processing; this demonstrates the feasibility of integrating PDMS devices into microfluidic chips [64]. As an example, tunable microlenses that are sensitive to chemical stimulation have been integrated in microfluidic chips. The focus of a PDMS microlens can be tuned by the injected microfluids.

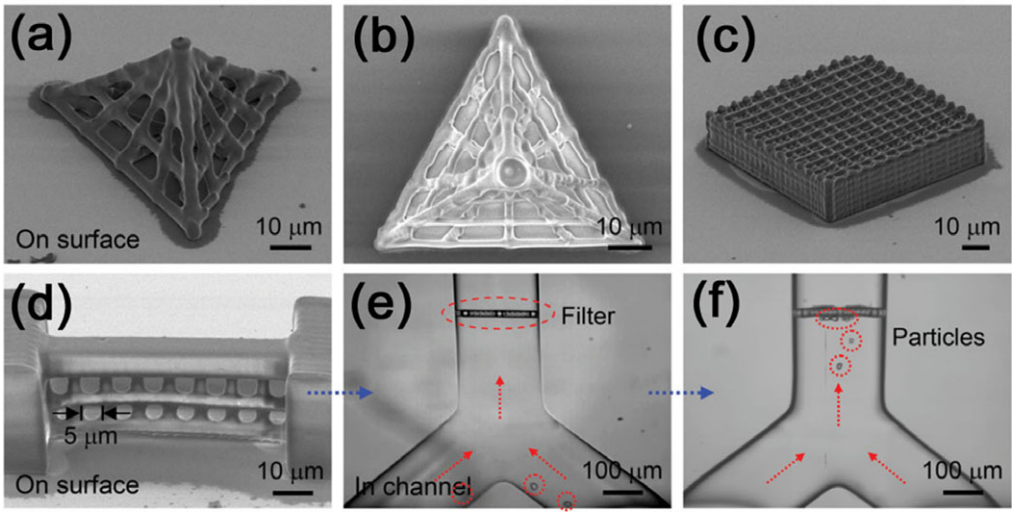

Figure 5 (a-c) SEM images of 3D complex cages and woodpile photonic crystals made by MPA. (d) SEM and (e), (f) optical images of 3D microsieves in channels. The shape and size of microsieves could be flexibly integrated according to target objects. (Reproduced with permission.[93] Copyright 2014, Wiley)

In addition to PDMS, various light-cured polymers are widely used for the on-chip processing of functional components [152]. Figure 5 shows some typical 3D functional microstructures of photopolymers that can be integrated with microfluidic chips, including micro-sieves with diameters of 5 μm [93]. Particles larger than 5 μm can be effectively separated (Fig. 5f). Exploiting the programmable processing, both the sizes and shapes of the micro-sieves can be designed and fabricated according to the target objects. For example, Wang *et al.* successfully fabricated vertical 3D micro-sieves with various pore shapes in a microchannel for shape/size-selective sieving and fish-scale-like microfilters as one-way valves [92]. Additional functions can be introduced by doping functional nanomaterials into the photopolymers [153–157]. For example, doping with magnetic NPs results in microdevices that can be remotely controlled by an external magnetic field [158, 159]. Sun *et al.* fabricated 3D photoluminescence CdS-polymer structures using the *in situ* synthesis of quantum dots (QDs) in a Cd^{2+}-doped polymethyacrylic acid network [99]. To date, photopolymers are the most general materials that have been used for OCLP. Various functional 3D polymer microstructures fabricated using laser processing can allow the creation of general microfluidic chips with additional functionalities [51].

3.3. Biomaterials

In addition to the synthetic photopolymers, some natural macromolecules are photosensitive also, which provides the possibility to fabricate some highly biocompatible microstructures for microfluidic chip functionalization. For example, 3D microstructures that consist of bovine serum albumin (BSA) [160–164], collagen [97, 165], silk fibroin [166], and many other proteins have been successfully fabricated using laser processing. Chen *et al.* fabricated 3D BSA structures using MPA (Fig. 6). An array of fluorescence-labeled BSA square prisms and cylinders and complex three square-based bridge structures have been demonstrated [167]. As shown in Fig. 6e, double bridge floors can be recognized clearly where the bridge is totally suspended. In this work, the authors found that the 3D BSA structures showed excellent cyto-compatibility for fibroblasts. Interestingly, the BSA microstructures were sensitive to pH change because the weak acidic and weak basic residues were protonated or deprotonated. In this case, the whole structure could shrink or swell due to the electrostatic interaction among the residues, which makes it possible to manipulate the microstructures by changing the surrounding pH value [67, 168]. Moreover, the as-obtained BSA structures allow further functionalization. For example, BSA could cross-link with some active proteins such as avidin that could specifically bind with biotin or biotin-labeled molecules, leading to applications in catalysis [66], detection [169], or tissue engineering [98, 170, 171].

In addition to BSA skeletons, some other proteins with very large numbers of active residues could also be solidified using laser irradiation with proper photosensitizers. Lin *et al.* integrated cross-linked AcmA' protein, which is known to bind specifically to Gram-positive bacteria, in bioprobe microfluidic chips for bacteria detecting [172]. Iosin *et al.* fabricated 3D enzyme reactors made of trypsin in microchannels using MPA [173]. With special bioactivities, collagen has been widely applied to construct scaffolds for tissue engineering [97, 165]. Additionally, cross-linked protein structures could be further modified using inorganic materials [174]. Sun *et al.* doped Ag and Au into silk fibroin structures that had a much greater Young's modulus and obtained conductive protein lines [166]. During photochemistry reactions, oxidizable groups of the silk fibroin acted as a bioreductant, and the protein molecules

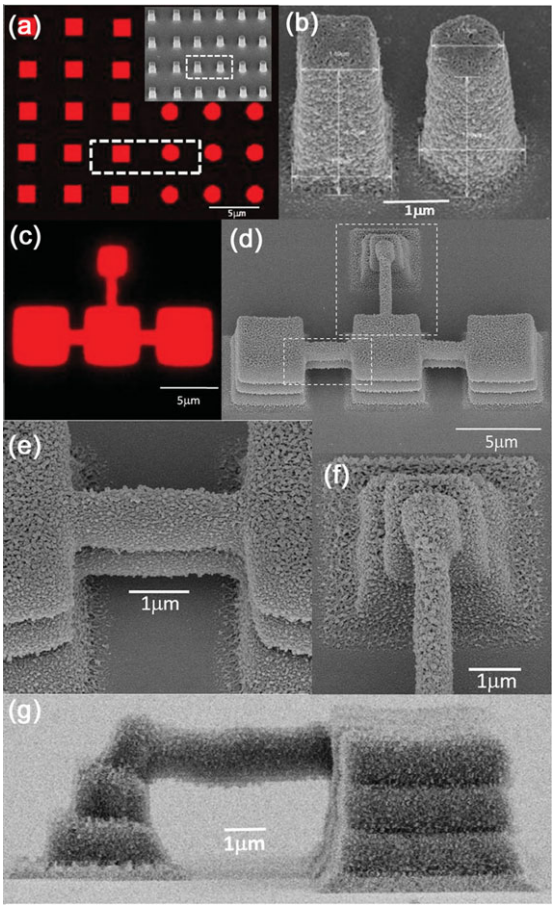

Figure 6 (a) An array of fluorescence labeled BSA square prisms and cylinders. Insert is the SEM image. (b) A magnified SEM of square prisms and cylinders. (c) A fluorescence labeled 3D BSA bridge. (d~g) SEM images of the complex bridge structure. (Reproduced with permission.[167] Copyright 2014, Wiley)

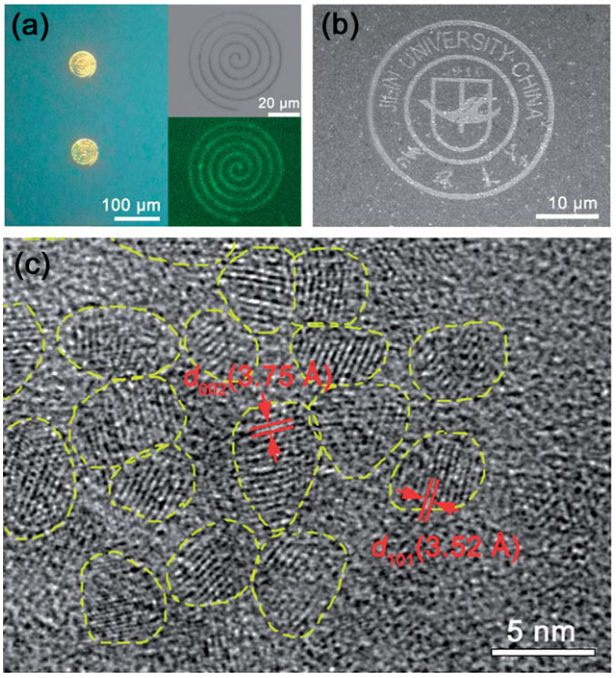

Figure 7 (a) Luminescence image of the CdTe QDs microstructures, the insets are the optical and confocal microscopic images of the circle structure. (b) SEM image of the badge of Jilin University made of QDs assemblies. (c) HTEM image of CdTe QDs assemblies. (Reproduced with permission.[68] Copyright 2013, Royal Society of Chemistry)

cross-linked. In this work, the doping density of Ag and Au could be easily controlled by adjusting the ion concentration or the pH value. It is reasonable that the OCLP of biomaterials could contribute to the development of multifunctional bio-chips. For instance, proteins containing groups that can be photo-oxidized, such as Tyr, Trp, His, Met, and Cys, can be cross-linked as 3D structures through MPA [67]. Therefore, various antibodies, antigens, enzymes, hormones and other proteins could be immobilized within the microfluidic chips to mimick the physiological functions. From this standpoint, OCLP of biomaterials demonstrates attractive prospects for bio-chips. However, during laser processing, parameters should be carefully optimized to prevent the deactivation of the proteins.

3.4. Nanomaterials

Taking advantage of photodynamic assembly technology, nanomaterials can also be assembled within microfluidic chips using OCLP [60]. As a typical example, Fig. 7 shows the femtosecond laser direct-writing-induced photodynamic assembly of CdTe QDs [68]. In this work, the absorption and luminescence spectra of CdTe QDs assemblies shifted only slightly compared with monodisperse CdTe QDs. This result indicates that the QDs did not grow into bulk material. High-resolution TEM image (Fig. 7c) of the assemblies confirms the aggregation of CdTe QDs. The QDs assemblies could be utilized for the on-chip detection of heavy metal ions.

In addition to semiconductor QDs, metal NPs (*e.g.*, Ag, Au) are other important types of nanomaterials that can be assembled using laser processing [101, 119]. Typically, Ag NPs can be assembled within microfluidic chips as microheaters for local temperature regulation [59]. The local temperature can achieve 54°C within 80 seconds when a voltage of 1 V is applied. Additionally, Ag assemblies can be used as electrodes due to their good conductivity [61]. Through designable laser processing, arbitrary morphological Ag electrodes can be fabricated. The integration of metallic micronanostructures within microfluidic chips is not limited to electrodes and heaters; they can be used as catalytic or surface-enhanced Raman spectroscopy (SERS) substrates for various applications [100, 111, 175], as is introduced in the following section.

It is well known that nanomaterials with controllable size, morphology and composition, have been widely applied in the medical field [176, 177], as well as in the fields of sensors [178], optics [179, 180], and catalysis [181].

With the development of the laser photodynamic assembly technology, more and more nanomaterials can now be flexibly assembled into microstructures, and act as functional components inside the microfluidic chips, revealing promising prospects in both basic research and practical applications [60]. However, the task of fabrication of these fine microstructures through the photodynamic assembly of nanomaterials remains a challenge. More importantly, preserving the size- and shape-dependent properties of these nanomaterials during the photodynamic assembly requires serious consideration [68].

4. Integration of multifunctional devices using OCLP

The development of multifunctional microfluidic chips requires the flexible integration of various functional components that can perform complex experimental procedures, such as sample separation, temperature control, and optofluidic detection. However, traditional 2D processing technologies cannot be used with microfluidic chips that are not flat. As an appealing alternative, OCLP technology permits the on-chip integration of various functional micro-nanostructures over a wide range of photosensitive materials and has great potential in chip functionalization. In this section, we introduce several representative examples including passive/active mixers, catalytic micro-reactors, micro-aquariums, sensors and optical components.

4.1. Micro-mixers

The mixing of microfluids is important for on-chip biochemical reactions. In general, when two or more streams are injected into micro-channels, they should be mixed rapidly before a reaction occurs. However, the laminar flow of microfluids makes it quite difficult to mix different liquids just through Brownian motion. Therefore, additional mixing devices are generally necessary for multifunctional microfluidic chips. To date, with the help of OCLP technology, various passive/active mixers have been successfully integrated with microfluidic chips [182]. As typical examples, Liao *et al.* fabricated passive microfluidic mixers in photosensitive glass using femtosecond laser microfabrication [183]. Two microchannels were twisted together. This disturbed stable laminar flow, leading to turbulent flow that accelerated the mixing of the microfluids. Additionally, Park *et al.* integrated 3D periodic nanoporous microstructures into a single microchannel to achieve the passive mixing of microfluids [184]. The nanoporous structure was fabricated using four-beam laser holographic lithography, which enables rapid fabrication of structures millimeters in length during one exposure. Nevertheless, the nanopores were so small that the streams were slowed down significantly, leading to non-obvious turbulent flow. To further improve the mixing efficiency, Lim *et al.* successfully developed a 3D crossing-manifold mixing structure within a microfluidic channel [57]. Several horizontal and vertical microcrossings achieved 90% mixing after 250 μm of passive stirring.

Compared with passive mixing, active mixers appear to be more efficient. As a typical example, Xia *et al.* synthesized photosensitive ferrofluids by doping 3-(trimethoxysilyl)propyl methacrylate (MPS) modified Fe_3O_4 NPs into a methyl acrylate photoresist and successfully fabricated a remotely controllable microturbine for active mixing [158,185]. As shown in Fig. 8, the microturbine was fabricated using FsLDW technology following a preprogrammed 3D structure; therefore the sizes, shapes, and even the angles of the microturbine's blades could be freely designed. Moreover, the microturbine could be placed at any location on the microfluidic chip. Under a rotating external magnetic field, this microturbine had a high rotating rate of 300 rpm, which guaranteed a high mixing efficiency.

4.2. Catalysis micro-reactors

Microfluidic chips are known to be efficient, high-throughout, sensitive, and reagent-saving reaction platforms that enable various chemical/biological reactions including synthesis, analysis, and catalysis [186]. In addition to the fabrication of functional microstructures, OCLP technology also enables the flexible integration of various catalysis microreactors. As a typical example, Narazaki *et al*, fabricated a TiO_2 catalysis microreactor using laser-induced superficial phase separation of Na_2O-TiO_2-SiO_2 glass [187]. During a nanosecond laser ablation and resolidification process, Na_2O and SiO_2 were evaporated, leaving TiO_2 bumps on the etched surface. With more pulses of radiation, the as-generated TiO_2 bumps joined together and formed a 3D TiO_2 micronetwork that can serve as a high-surface-area catalyst for the photocatalytic decomposition of methylene blue. The *in situ* laser production of TiO_2 photocatalysts provides a simple method for facile integration of photocatalytic microreactors.

In addition to TiO_2, Ag NPs can also be flexibly assembled into microfluidic chips and serve as catalysts. As shown in Fig. 9, FsLDW-induced photoreduction of Ag^+ directly leads to the formation of hierarchical Ag structures of upright nanoplates and tiny particles on the surfaces [175]. The hierarchical nanostructures increased the specific surface area and had high activity for the catalytic reduction of 4-nitrophenol (4-NP) to 4-aminophenol (4-AP). As shown in Fig. 9d, the micro-region absorption peak of 4-NP at 380 nm gradually decreased with the reaction time, and the conversion of 4-NP reached almost 100% after only 7 minutes. Figure 9e shows the dependence of the reaction conversion rate on the flow velocity. Obviously, a relatively low flow rate would prolong the interaction time between reactants and the Ag catalysts and accordingly lead to high conversion efficiency.

The OCLP of metallic catalysts is not limited to Ag. Zarzar *et al.* reported a MPA fabrication of Pt-protein compound structures within a 3D microreactor [100]. As soon

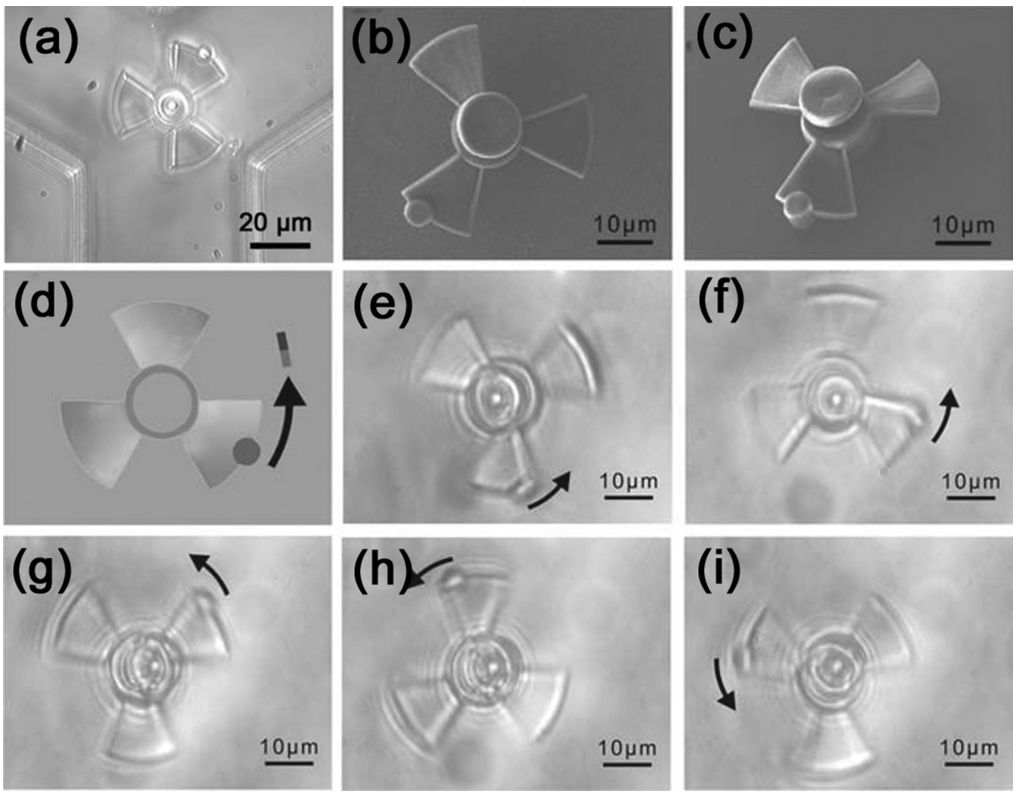

Figure 8 (a) Optical image of microturbine in a Y-shape channel for active mixing two streams by introducing turbulent flow. (b, c) SEM images of the microturbine. (d) Top view scheme for rotation. (e-i) Optical images of a rotating microturbine. (Reproduced with permission.[158] Copyright 2010, Wiley)

as H_2O_2 was introduced into the reactor, O_2 was released. Consequently, the gas bubbles drove the liquid and the microspecies in the solution in a manner similar to a pump. This Pt-protein catalytic microreactor could be equipped into microfluidic chips as motive power.

4.3. Micro-aquariums

Microorganisms are small in size and some move very quickly; therefore, macroscopic containers, such as petri dishes, are too large to confine them when studying their behavior under a microscope. Recently, 3D glass microfluidic chips machined using femtosecond laser microfabrication have been applied to culture microorganisms [188–191]. As a typical example, Hanada *et al.* introduced *Euglena gracilis* into 3D channels (Fig. 10a) slightly larger than the small creatures to observe how they whipped their flagella [192]. Due to the confined space, *Euglena gracilis* could move only along the 3D channels; thus, continuous 3D observation could be achieved (Fig. 10b). With the help of these 3D micro-aquariums, the authors found that *Euglena gracilis* whipped their flagellums differently when moving away from strong light compared with swimming in a straight line. Additionally, for the first time, the front view of swimming *Euglena gracilis* was observed when they moved upward in the reservoir.

Taking advantage of the designable OCLP, Hanada *et al.* further fabricated more complex chips to investigate the gliding mechanism of *Phormidium* in detail [193, 194]. Using an as-fabricated T-channel, they found that a seedling root might release something that could attract *Phormidium*. To make this phenomenon clear, they designed a CO_2 slow-release chip that contained three corners; a seedling root and a *Phormidium* were introduced at two corners, and the slow-release corner was filled with CO_2 solution. When the CO_2 concentration was low, *Phormidium* would move to the seedling root, whereas when a high concentration was introduced, *Phormidium* would move in the direction of the CO_2 solution. These results demonstrated that it was the CO_2 released by the seedling root that attracted *Phormidium* to glide. Additionally, the same team found that light was required for the gliding. To confirm this result, they modified the photosensitive glass using femtosecond laser treatments and used it to filter light. When enough filters were fabricated on the glass channels, no further gliding of *Phormidium* was observed. These works indicate that designable femtosecond laser processing makes it possible to develop functional microfluidic chips as innovative experimental platforms for biology research.

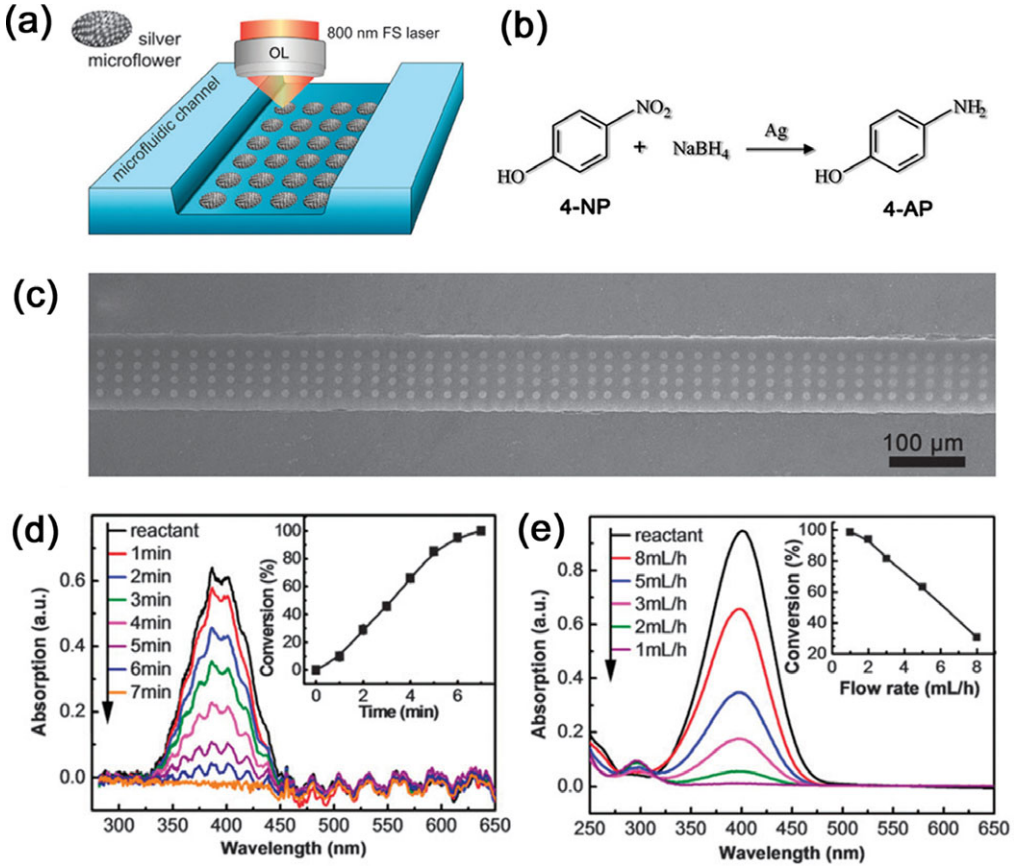

Figure 9 (a) Scheme and (c) SEM images of Ag nanoplates integrated in microchannel. (b) Catalysis reaction carried out in the catalysis microreactors. (d) Micro-region absorption spectrums of the microfluids during the rection. Insert is kinetic study of the reaction. (e) Absorption spectrums of products under different flow rates. Insert is kinetic study of the reaction. (Reproduced with permission.[175] Copyright 2012, Royal Society of Chemistry)

4.4. Cell counters

Counting cells is significant for biology research and disease diagnosis. In clinical applications, counting is typically performed by flow cytometry, which is expensive and inefficient. Currently, with the rapid progress of OCLP technology, microoptic components can readily be integrated with microfluidic chips for on-chip cell counting [195–197]. As a typical example, Wu *et al.* first machined photosensitive glass to fabricate a microfluidic channel using femtosecond laser pulses, then integrated a polymer microlens into the chip using MPA, as shown in Fig. 11 [198]. When a cell passed through the light path of the microlens, a signal was recorded. In this way, the microlens-equipped microchannel worked as a cell counter. To avoid mis-counting, Wu *et al.* integrated a microlens array along the cross-line of the channel for parallel cell counting, and 93% of the cells were counted; some cells passed between the two microlenses and were missed. To make further improvements, the authors fabricated M-shaped confining walls through MPA for the microlens array [199]. In this way, all of the cells were confined to pass directly through the light path of microlens achieving a 100% success rate.

However, when non-uniform or dense cell liquids pass through such cell counters, the channels might be blocked. Recently, Lv *et al.* created an optofluidic-microfluidic twin-channel system [200]. In the upper channel, a microlens was integrated using FsLDW, and the bottom channel allowed the cells to pass, offering a good solution for cell blocking. Additionally, Paiè *et al.* reported a straightforward 3D hydrodynamic focusing microfluidic chip fabricated using femtosecond laser microfabrication; this chip reduced the blocking problem dramatically [81]. These authors fabricated a center microchannel with four parallel surrounding channels, and the five microchannels finally converged as a wide channel into which a waveguide was integrated using femtosecond laser modification of the refractive index of the glass. In their work, diluted blood was delivered through the center channel and liquid without cells was introduced into the surrounding channels. Based on the hydrodynamic focusing effect, when the five streams converged, the diluted blood would flow in the center of the wide channel without a blocking problem. By adjusting the flux of the five streams, cells could pass in a fine stream directly through the light path of the integrated waveguide. In this way, correct and fast cell counting could be achieved.

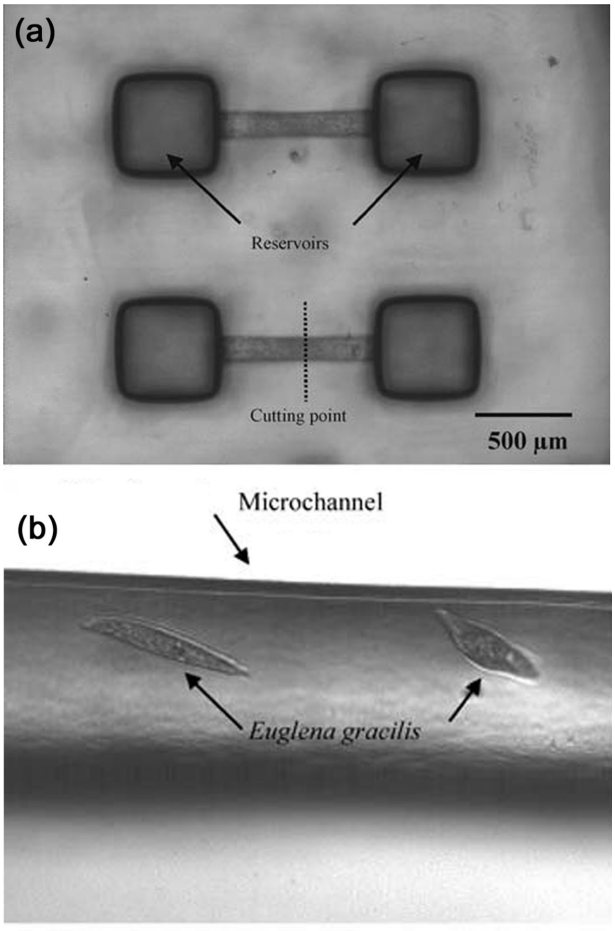

Figure 10 (a) 3D glass microaquariums used for observing *Euglena gracilis*. (b) Optical image of *Euglena gracilis* limited in the channels. (Reproduced with permission.[192] Copyright 2008, Springer)

4.5. SERS sensors

As an advanced optofluidic detection technology, on-chip SERS detection has emerged as a promising tool that features label-free fingerprint Raman spectra of reagents with ultrahigh sensitivity [201–203]. The combination of the SERS technique with microfluidic chips requires flexible integration of metal plasmonic structures with the microfluidic chips. However, it is challenging for general 2D processing methods to construct SERS substrates within a microchannel which is not flat. At first, noble-metal nanocolloids as flowing SERS substrates were injected into microfluidic chips for SERS detection [204]. Currently, with the help of OCLP technology, Ag and Au hierarchical micronanostructures can be well integrated with microfluidic chips [205–208]. As a typical example, Xu *et al.* fabricated Ag SERS substrates within a microfluidic channel using femtosecond laser direct-writing-induced photoreduction of Ag^+ [65]. By exploiting the "direct writing" feature, the Ag SERS substrates were well integrated within the microfluidic chips by patterning the Ag structures into various shapes and at any desired position, as shown in Fig. 12a [111]. The resultant SERS substrates were constructed using hierarchical micronanostructures that consisted of oriented Ag nanoplates with tiny NPs decorating (Fig. 12b). The formation of such hierarchical structures can be attributed to the MPA-induced photoreduction of Ag^+ and the subsequent photodynamic assembly of the as-formed Ag NPs. In principle, Ag NPs were assembled using SPR-enhanced optical tweezers along the polarized direction of the laser. In this process, electrostatic forces between the pre-formed nanoplates and the free Ag NPs, coupled with the gradient forces produced by the optical tweezers, induced the photodynamic assembly process, forming an

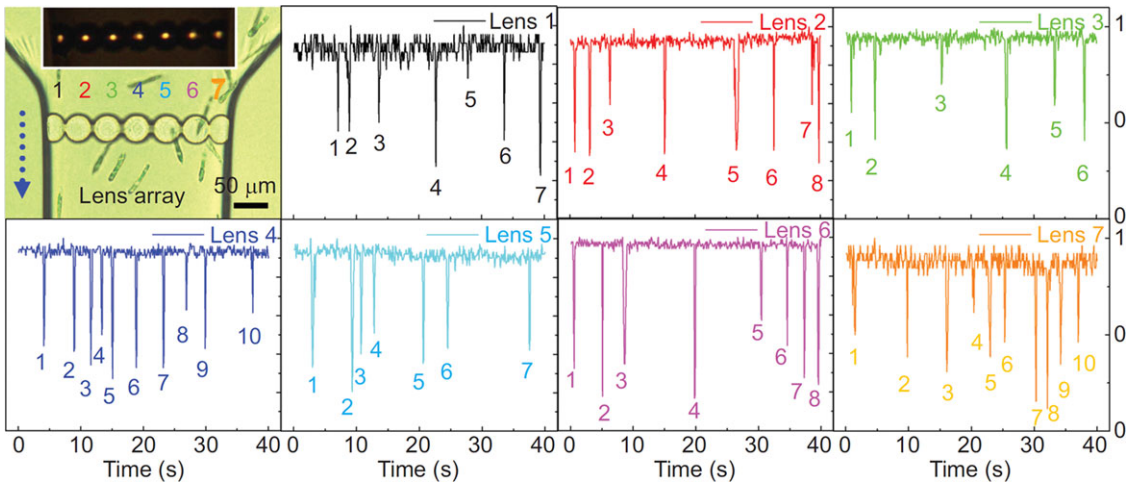

Figure 11 Optical images of microlens array integrated in glass channel and optical signals of every lens in the array from lens 1 to lens 7, when counting cells. Inset image presents focal spots produced by the microlens array. (Reproduced with permission.[198] Copyright 2015, Nature Publishing Group)

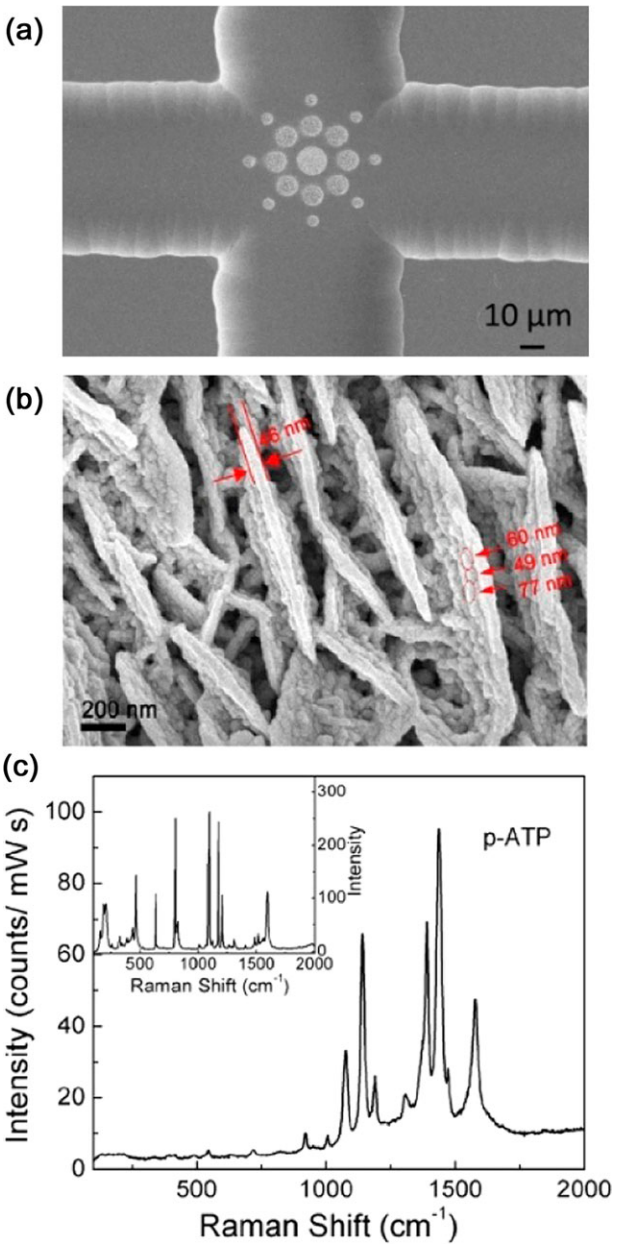

Figure 12 (a) Ag SERS substrates integrated in a microchannel. (b) SEM image of the detail micronanostructures, upright nanoplates decorated with many NPs. (c) A SERS signal of p-ATP molecules. The normalized intensity was gained by dividing the initial value by 10 mW and 10 s. (Reproduced with permission.[111] Copyright 2014, American Chemical Society)

oriented Ag nanoplate and Ag NPs hierarchical structures. Due to the presence of abundant "hot-spots", a SERS enhancement factor as high as 10^{11} was achieved (Fig. 12c). OCLP makes it possible to integrate SERS substrates with microfluidic chips in a controlled manner, which further contributes to the post-functionalization of microfluidic chips and optofluidic SERS detection.

5. Conclusions and future perspective

In recent decades, microfluidic chips have widely investigated in both fundamental science and practical applications. They have demonstrated great potential for blood analysis, water monitoring, and tissue engineering. In the development of microfluidic devices, conventional 2D micro/nanofabrication technologies that have been widely used in the semiconductor industry contributed greatly to the initial processing methods. However, the 2D processing somewhat limits the further functionalization of microfluidic chips because the microchannel networks are nonplanar substrates. Therefore, 3D methods that permit the on-chip integration of multifunctional components based on a wide range of materials are urgently needed. Recently, laser fabrication technologies that enable 3D processing of various functional materials have emerged as an appealing alternative to achieve this goal. In this review paper, we summarized the recent development of OCLP technologies. Typical photochemical/photophysical schemes were introduced, including both subtraction-type and addition-type processing, such as laser ablation, laser induced photopolymerization, laser induced photoreduction and photodynamic assembly, as well as a wide range of laser processable materials, including glass, photopolymers, metals, biomaterials and even nanoparticles. Several attractive multifunctional components that impart additional functionalities to conventional microfluidic chips were comprehensively reviewed.

Compared to the conventional 2D lithographic technology that has been widely employed for chip fabrication, OCLP has several unique advantages. For example, ultra-short pulse laser microfabrication is capable of machining complex 3D microchannels in glass or polymers, making the 3D chips development possible; MPA enables 3D prototyping of various functional structures at any desired position in a microfluidic channel, providing a way to integrate complex components on nonplanar microfluidic channels. Specifically, the laser induced photodynamic assembly technique allows for the patternable assembly of various NPs into functional devices, bridging the gap between nanomaterials and microdevices. Additionally, from a materials standpoint, OCLP is also promising in chip functionalization, since there are so many materials that can be potentially processed in this manner. Nowadays, functional components based on different materials could be readily integrated with microfluidic chips. For instance, general photopolymers could be doped with fluorescent, magnetic, or conductive nanomaterials for chip functionalization; for biological applications, photosensitive biomaterials, such as BSA, enzymes, and collagen could be processed, revealing great potential for on-chip biological analysis, tissue engineering and even organ-on-a-chip systems. Moreover, OCLP technology is compatible with the conventional 2D processing technologies. Functional components based on different materials could be post-equipped with a given microfluidic chip. With the rapid development of laser processing technology, fabricating accuracy of the ultrafast laser processing has been significantly improved to the

order of tens of nanometers, far beyond the optical diffraction limit, making it possible to functionalize microfluidic chips with nanoscale components.

However, OCLP also has several shortcomings. Compared with wafer-level fabrication, point-to-point processing has a relatively low efficiency. To address this issue, one possible solution would be multiple-beam parallel scanning [209, 210]. Alternatively, the use of laser holography also enables rapid processing [206–208, 211]; 2D/3D periodic microstructures at a centimeter scale could be fabricated within a few seconds. Currently, OCLP is still in the early stage of development. With the progress of laser processing technologies and materials science, additional photosensitive materials could be used in laser processing, and OCLP would grow in sophistication and act as an enabler of multifunctional microfluidic chips.

Acknowledgements. The authors would like to acknowledge the National Natural Science Foundation of China (NSFC) and National Basic Research Program of China (973 program) under grants #61522503, #61376123, #2014CB921302, #61435005, and #61590930 for support.

Received: 9 May 2016, **Revised:** 23 December 2016, **Accepted:** 13 February 2017

Published online: 6 March 2017

Key words: Microfluidic chips, on-chip laser processing (OCLP), photosensitive materials, integration, femtosecond laser.

References

[1] N. Cherkasov, A. O. Ibhadon, and E. V. Rebrov, Lab Chip **15**, 1952–1960 (2015).
[2] J. Parmar, S. Jang, L. Soler, D. P. Kim, and S. Sanchez, Lab Chip **15**, 2352–2356 (2015).
[3] H. Zhao, J. H. Xu, T. Wang, and G. S. Luo, Lab Chip **14**, 1901–1906 (2014).
[4] P. T. Lin, S. W. Kwok, H. Y. Lin, V. Singh, L. C. Kimerling, G. M. Whitesides, and A. Agarwal, Nano Lett. **14**, 231–238 (2014).
[5] B. Abecassis, C. Cottin-Bizonne, C. Ybert, A. Ajdari, and L. Bocquet, Nat. Mater. **7**, 785–789 (2008).
[6] R. Vilensky, M. Bercovici, and E. Segal, Adv. Funct. Mater. **25**, 6725–6732 (2015).
[7] F. Kong, X. Zhang, H. Zhang, X. Qu, D. Chen, M. Servos, E. Mäkilä, J. Salonen, H. A. Santos, M. Hai, and D. A. Weitz, Adv. Funct. Mater. **25**, 3330–3340 (2015).
[8] B. Xiong, K. Ren, Y. Shu, Y. Chen, B. Shen, and H. Wu, Adv. Mater. **26**, 5525–5532 (2014).
[9] Y. Zhao, D. Chen, H. Yue, M. M. Spiering, C. Zhao, S. J. Benkovic, and T. J. Huang, Nano Lett. **14**, 1952–1960 (2014).
[10] O. Frey, P. M. Misun, D. A. Fluri, J. G. Hengstler, and A. Hierlemann, Nat. Commun. **5**, 4250 (2014).
[11] S. Tasoglu, E. Diller, S. Guven, M. Sitti, and U. Demirci, Nat. Commun. **5**, 3124 (2014).
[12] Z. Cao, C. Chen, B. He, K. Tan, and C. Lu, Nat. Methods **12**, 959–962 (2015).
[13] R. F. Service, Science **338**, 731–731 (2012).
[14] S. Nahavandi, S. Y. Tang, S. Baratchi, R. Soffe, S. Nahavandi, K. Kalantar-zadeh, A. Mitchell, and K. Khoshmanesh, Small **10**, 4810–4826 (2014).
[15] G. G. Giobbe, F. Michielin, C. Luni, S. Giulitti, S. Martewicz, S. Dupont, A. Floreani, and N. Elvassore, Nat. Methods **12**, 637–640 (2015).
[16] M. Otten, W. Ott, M. A. Jobst, L. F. Milles, T. Verdorfer, D. A. Pippig, M. A. Nash, and H. E. Gaub, Nat. Methods **11**, 1127–1130 (2014).
[17] Y. S. Torisawa, C. S. Spina, T. Mammoto, A. Mammoto, J. C. Weaver, T. Tat, J. J. Collins, and D. E. Ingber, Nat. Methods **11**, 663–669 (2014).
[18] C. Franco and H. Gerhardt, Nature **488**, 465–466 (2012).
[19] D. Huh, B. D. Matthews, A. Mammoto, M. Montoya-Zavala, H. Y. Hsin, and D. E. Ingber, Science **328**, 1662–1668 (2010).
[20] S. S. Acimovic, M. A. Ortega, V. Sanz, J. Berthelot, J. L. Garcia-Cordero, J. Renger, S. J. Maerkl, M. P. Kreuzer, and R. Quidant, Nano Lett. **14**, 2636–2641 (2014).
[21] R. J. Kimmerling, G. Lee Szeto, J. W. Li, A. S. Genshaft, S. W. Kazer, K. R. Payer, J. de Riba Borrajo, P. C. Blainey, D. J. Irvine, A. K. Shalek, and S. R. Manalis, Nat. Commun. **7**, 10220 (2016).
[22] H. Shao, J. Chung, K. Lee, L. Balaj, C. Min, B. S. Carter, F. H. Hochberg, X. O. Breakefield, H. Lee, and R. Weissleder, Nat. Commun. **6**, 6999 (2015).
[23] E. Stern, A. Vacic, N. K. Rajan, J. M. Criscione, J. Park, B. R. Ilic, D. J. Mooney, M. A. Reed, and T. M. Fahmy, Nat. Nanotechnol. **5**, 138–142 (2010).
[24] M. K. Sarvothaman, K. S. Kim, B. Seale, P. M. Brodersen, G. C. Walker, and A. R. Wheeler, Adv. Funct. Mater. **25**, 506–515 (2015).
[25] A. Albanese, A. K. Lam, E. A. Sykes, J. V. Rocheleau, and W. C. Chan, Nat. Commun. **4**, 2718 (2013).
[26] A. H. Ng, M. Dean Chamberlain, H. Situ, V. Lee, and A. R. Wheeler, Nat. Commun. **6**, 7513 (2015).
[27] E. K. Sackmann, A. L. Fulton, and D. J. Beebe, Nature **507**, 181–189 (2014).
[28] R. J. Shilton, V. Mattoli, M. Travagliati, M. Agostini, A. Desii, F. Beltram, and M. Cecchini, Adv. Funct. Mater. **25**, 5895–5901 (2015).
[29] B. Herranz-Blanco, D. Liu, E. Mäkilä, M. A. Shahbazi, E. Ginestar, H. Zhang, V. Aseyev, V. Balasubramanian, J. Salonen, J. Hirvonen, and H. A. Santos, Adv. Funct. Mater. **25**, 1488–1497 (2015).
[30] P. M. Valencia, O. C. Farokhzad, R. Karnik, and R. Langer, Nat. Nanotechnol. **7**, 623–629 (2012).
[31] C. T. Riche, E. J. Roberts, M. Gupta, R. L. Brutchey, and N. Malmstadt, Nat. Commun. **7**, (2016).
[32] J. M. del Rio Martinez, E. Zaitseva, S. Petersen, G. Baaken, and J. C. Behrends, Small **11**, 119–125 (2015).
[33] S. Rajauria, C. Axline, C. Gottstein, and A. N. Cleland, Nano Lett. **15**, 469–475 (2015).
[34] A. M. Skelley, O. Kirak, H. Suh, R. Jaenisch, and J. Voldman, Nat. Methods **6**, 147–152 (2009).
[35] H. J. Yoon, T. H. Kim, Z. Zhang, E. Azizi, T. M. Pham, C. Paoletti, J. Lin, N. Ramnath, M. S. Wicha, D. F. Hayes, D. M. Simeone, and S. Nagrath, Nat. Nanotechnol. **8**, 735–741 (2013).

[36] S. Nagrath, L. V. Sequist, S. Maheswaran, D. W. Bell, D. Irimia, L. Ulkus, M. R. Smith, E. L. Kwak, S. Digumarthy, A. Muzikansky, P. Ryan, U. J. Balis, R. G. Tompkins, D. A. Haber, and M. Toner, Nature **450**, 1235–1239 (2007).
[37] M. Kang, W. Park, S. Na, S. M. Paik, H. Lee, J. W. Park, H. Y. Kim, and N. L. Jeon, Small **11**, 2789–2797 (2015).
[38] M. Werner, R. Palankar, L. Arm, R. Hovius, and H. Vogel, Small **11**, 2607–2613 (2015).
[39] V. Murlidhar, M. Zeinali, S. Grabauskiene, M. Ghannad-Rezaie, M. S. Wicha, D. M. Simeone, N. Ramnath, R. M. Reddy, and S. Nagrath, Small **10**, 4895–4904 (2014).
[40] T. Wienhold, S. Kraemmer, S. F. Wondimu, T. Siegle, U. Bog, U. Weinzierl, S. Schmidt, H. Becker, H. Kalt, T. Mappes, S. Koeber, and C. Koos, Lab Chip **15**, 3800–3806 (2015).
[41] S. Wang, K. Liu, J. Liu, Z. T. Yu, X. Xu, L. Zhao, T. Lee, E. K. Lee, J. Reiss, Y. K. Lee, L. W. Chung, J. Huang, M. Rettig, D. Seligson, K. N. Duraiswamy, C. K. Shen, and H. R. Tseng, Angew. Chem. Int. Ed. **50**, 3084–3088 (2011).
[42] H. Cheng, C. Han, Z. Xu, J. Liu, Y. Wang, Food Anal. Methods **7**, 2153–2162 (2014).
[43] M. S. Kim, T. S. Sim, Y. J. Kim, S. S. Kim, H. Jeong, J. M. Park, H. S. Moon, S. I. Kim, O. Gurel, S. S. Lee, J. G. Lee, and J. C. Park, Lab Chip **12**, 2874–2880 (2012).
[44] L. Lallement, C. Gosse, C. Cardinaud, M. C. Peignon-Fernandez, and A. Rhallabi, J. Vac. Sci. Technol. A **28**, 277 (2010).
[45] M. B. Mikkelsen, A. A. Letailleur, E. Sondergard, E. Barthel, J. Teisseire, R. Marie, and A. Kristensen, Lab Chip **12**, 2662–267 (2012).
[46] A. E. Vasdekis, M. J. Wilkins, J. W. Grate, R. T. Kelly, A. E. Konopka, S. S. Xantheas, and T. M. Chang, Lab Chip **14**, 2072–2080 (2014).
[47] J. Wu, R. Chantiwas, A. Amirsadeghi, S. A. Soper, and S. Park, Lab Chip **11**, 2984–2989 (2011).
[48] R. Ramji, C. F. Cheong, H. Hirata, A. R. Rahman, and C. T. Lim, Small **11**, 943–951 (2015).
[49] Y. Wang, J. Balowski, C. Phillips, R. Phillips, C. E. Sims, and N. L. Allbritton, Lab Chip **11**, 3089–3097 (2011).
[50] M. E. Wilson, N. Kota, Y. Kim, Y. Wang, D. B. Stolz, P. R. LeDuc, and O. B. Ozdoganlar, Lab Chip **11**, 1550–1555 (2011).
[51] B. B. Xu, Y. L. Zhang, H. Xia, W. F. Dong, H. Ding, and H. B. Sun, Lab Chip **13**, 1677–1690 (2013).
[52] K. Ren, J. Zhou, and H. Wu, Accounts Chem. Res. **46**, 2396–2406 (2013).
[53] P. F. O'Neill, A. Ben Azouz, M. Vazquez, J. Liu, S. Marczak, Z. Slouka, H. C. Chang, D. Diamond, and D. Brabazon, Biomicrofluidics **8**, 052112 (2014).
[54] K. Sugioka, J. Xu, D. Wu, Y. Hanada, Z. Wang, Y. Cheng, and K. Midorikawa, Lab Chip **14**, 3447–3458 (2014).
[55] K. Sugioka, and Y. Cheng, Appl. Phys. A **114**, 215–221 (2013).
[56] M. Malinauskas, M. Farsari, A. Piskarskas, and S. Juodkazis, Phys. Rep. **533**, 1–31 (2013).
[57] T. W. Lim, Y. Son, Y. J. Jeong, D. Y. Yang, H. J. Kong, K. S. Lee, and D. P. Kim, Lab Chip **11**, 100–103 (2011).
[58] Y. He, B. L. Huang, D. X. Lu, J. Zhao, B. B. Xu, R. Zhang, X. F. Lin, Q. D. Chen, J. Wang, Y. L. Zhang, and H. B. Sun, Lab Chip **12**, 3866–3869 (2012).
[59] B. B. Xu, H. Xia, L. G. Niu, Y. L. Zhang, K. Sun, Q. D. Chen, Y. Xu, Z. Q. Lv, Z. H. Li, H. Misawa, and H. B. Sun, Small **6**, 1762–1766 (2010).
[60] H. Wang, Y. L. Zhang, H. Xia, Q. D. Chen, K. S. Lee, and H. B. Sun, Nanoscale Horiz. (2016).
[61] H. Wang, S. Liu, Y. L. Zhang, J. N. Wang, L. Wang, H. Xia, Q. D. Chen, H. Ding, and H. B. Sun, Sci. Technol. Adv. Mater. **16**, 024805 (2016).
[62] E. F. M. Gabriel, W. K. T. Coltro, and C. D. Garcia, Electrophoresis **35**, 2325–2332 (2014).
[63] S. Prakash and S. Kumar, Int. J. Precis. Eng. Man. **16**, 361–366 (2015).
[64] D. X. Lu, Y. L. Zhang, D. D. Han, H. Wang, H. Xia, Q. D. Chen, H. Ding, and H. B. Sun, J. Mater. Chem. C **3**, 1751–1756 (2015).
[65] B. B. Xu, Z. C. Ma, L. Wang, R. Zhang, L. G. Niu, Z. Yang, Y. L. Zhang, W. H. Zheng, B. Zhao, Y. Xu, Q. D. Chen, H. Xia, and H. B. Sun, Lab Chip **11**, 3347–3351 (2011).
[66] R. Allen, R. Nielson, D. D. Wise, and J. B. Shear, Anal. Chem. **77**, 5089–5095 (2005).
[67] Y. L. Sun, W. F. Dong, R. Z. Yang, X. Meng, L. Zhang, Q. D. Chen, and H. B. Sun, Angew. Chem. Int. Ed. **51**, 1558–1562 (2012).
[68] B. B. Xu, Y. L. Zhang, R. Zhang, L. Wang, X. Z. Xiao, H. Xia, Q. D. Chen, and H. B. Sun, J. Mater. Chem. C **1**, 4699 (2013).
[69] R. R. Gattass and E. Mazur, Nat. Photonics **2**, 219–225 (2008).
[70] Y. Liao, Y. Cheng, C. Liu, J. Song, F. He, Y. Shen, D. Chen, Z. Xu, Z. Fan, X. Wei, K. Sugioka, and K. Midorikawa, Lab Chip **13**, 1626–1631 (2013).
[71] K. R. Kim, H. J. Kim, H. I. Choi, K. S. Shin, S. H. Cho, and B. D. Choi, Microelectron. Eng. **140**, 1–5 (2015).
[72] S. Bonk, P. Oldorf, R. Peters, W. Baumann, and J. Gimsa, Micromachines **6**, 364–374 (2015).
[73] M. Malinauskas, S. Rekštytė, L. Lukoševičius, S. Butkus, E. Balčiūnas, M. Pečiukaitytė, D. Baltriukienė, V. Bukelskienė, A. Butkevičius, P. Kucevičius, V. Rutkūnas, and S. Juodkazis, Micromachines **5**, 839–858 (2014).
[74] C. K. Chung and K. Z. Tu, Microsyst. Technol. **20**, 1987–1992 (2013).
[75] S. F. Tseng, M. F. Chen, W. T. Hsiao, C. Y. Huang, C. H. Yang, and Y. S. Chen, Opt. Lasers Eng. **57**, 58–63 (2014).
[76] Y. Cheng, H. L. Tsai, K. Sugioka, and K. Midorikawa, Appl. Phys. A **85**, 11–14 (2006).
[77] C. H. Lin, L. Jiang, Y. H. Chai, H. Xiao, S. J. Chen, and H. L. Tsai, Appl. Phys. A **97**, 751–757 (2009).
[78] B. N. Chichkov, C. Momma, S. Nolte, F. Alvensleben, and A. Tünnermann, Appl. Phys. A **63**, 109–115 (1996).
[79] N. M. Bulgakova, R. Stoian, and A. Rosenfeld, Quantum Electron. **40**, 966–985 (2010).
[80] F. He, Y. Liao, J. Lin, J. Song, L. Qiao, Y. Cheng, and K. Sugioka, Sensors **14**, 19402–19440 (2014).
[81] P. Paie, F. Bragheri, R. M. Vazquez, and R. Osellame, Lab Chip **14**, 1826–1833 (2014).
[82] J. Huft, D. J. Da Costa, D. Walker, and C. L. Hansen, Lab Chip **10**, 2358–2365 (2010).
[83] S. Kawata, H. B. Sun, T. Tanaka, and K. Takada, Nature **412**, 697–698 (2001).

[84] A. Ovsianikov, J. Viertl, B. Chichkov, M. Oubaha, B. MacCraith, I. Sakellari, A. Giakoumaki, D. Gray, M. Vamvakaki, M. Farsari, and C. Fotakis, ACS Nano **2**, 2257–2262 (2008).
[85] B. Kaehr, J. B. Shear, and P. Natl. Acad. Sci USA **105**, 8850–8854 (2008).
[86] L. D. Zarzar, P. Kim, M. Kolle, C. J. Brinker, J. Aizenberg, and B. Kaehr, Angew. Chem. Int. Ed. **50**, 9356–9360 (2011).
[87] H. B. Sun and S. Kawata, Cheminform **36**, 169–273 (2005).
[88] Y. Tian, Y. L. Zhang, H. Xia, L. Guo, J. F. Ku, Y. He, R. Zhang, B. Z. Xu, Q. D. Chen, and H. B. Sun, Phys. Chem. Chem. Phys. **13**, 4835–4838 (2011).
[89] T. Tanaka, H. B. Sun, and S. Kawata, Applied Physics Letters **80**, 312 (2002).
[90] Y. L. Zhang, Q. D. Chen, H. Xia, and H. B. Sun, Nano Today **5**, 435–448 (2010).
[91] D. Wu, Q. D. Chen, L. G. Niu, J. N. Wang, J. Wang, R. Wang, H. Xia, and H. B. Sun, Lab Chip **9**, 2391–2394 (2009).
[92] J. Wang, Y. He, H. Xia, L. G. Niu, R. Zhang, Q. D. Chen, Y. L. Zhang, Y. F. Li, S. J. Zeng, J. H. Qin, B. C. Lin, and H. B. Sun, Lab Chip **10**, 1993–1996 (2010).
[93] D. Wu, S. Z. Wu, J. Xu, L. G. Niu, K. Midorikawa, and K. Sugioka, Laser Photonics Rev. **8**, 458–467 (2014).
[94] A. Ovsianikov, V. Mironov, J. Stampf, and R. Liska, Expert Rev. Med. Devices **9**, 613–633 (2012).
[95] R. G. Wylie, S. Ahsan, Y. Aizawa, K. L. Maxwell, C. M. Morshead, and M. S. Shoichet, Nat. Mater. **10**, 799–806 (2011).
[96] S. Basu, L. P. Cunningham, G. D. Pins, K. A. Bush, R. Taboada, A. R. Howell, J. Wang, and P. J. Campagnola, Biomacromolecules **6**, 1465–1474 (2005).
[97] P. J. Su, Q. A. Tran, J. J. Fong, K. W. Eliceiri, B. M. Ogle, and P. J. Campagnola, Biomacromolecules **13**, 2917–2925 (2012).
[98] K. Gomi, M. Kanazashi, D. Lickorish, T. Arai, and J. E. Davies, J. Biomed. Mater. Res. A **71**, 602–607 (2004).
[99] Z. B. Sun, X. Z. Dong, W. Q. Chen, S. Nakanishi, X. M. Duan, and S. Kawata, Adv. Mater. **20**, 914–919 (2008).
[100] L. D. Zarzar, B. S. Swartzentruber, J. C. Harper, D. R. Dunphy, C. J. Brinker, J. Aizenberg, and B. Kaehr, J. Am. Chem. Soc. **134**, 4007–4010 (2012).
[101] C. N. LaFratta, D. Lim, K. O'Malley, T. Baldacchini, and J. T. Fourkas, Chem. Mater. **18**, 2038–2042 (2006).
[102] W. E. Lu, M. L. Zheng, W. Q. Chen, Z. S. Zhao, and X. M. Duan, Phys. Chem. Chem. Phys. **14**, 11930–11936 (2012).
[103] W. E. Lu, Y. L. Zhang, M. L. Zheng, Y. P. Jia, J. Liu, X. Z. Dong, Z. S. Zhao, C. B. Li, Y. Xia, T. C. Ye, and X. M. Duan, Opt. Mater. Express **3**, 1660 (2013).
[104] Z. C. Ma, Q. D. Chen, B. Han, X. Q. Liu, J. F. Song, and H. B. Sun, Sci. Rep. **5**, 17712 (2015).
[105] T. Tanaka, A. Ishikawa, and S. Kawata, Appl. Phys. Lett. **88**, 081107 (2006).
[106] Y. Y. Cao, N. Takeyasu, T. Tanaka, X. M. Duan, and S. Kawata, Small **5**, 1144–1148 (2009).
[107] Y. Y. Cao, X. Z. Dong, N. Takeyasu, T. Tanaka, Z. S. Zhao, X. M. Duan, and S. Kawata, Appl. Phys. A **96**, 453–458 (2009).
[108] M. R. Langille, J. Zhang, and C. A. Mirkin, Angew. Chem. Int. Ed. **50**, 3543–3547 (2011).
[109] J. Zhang, S. Li, J. Wu, G. C. Schatz, and C. A. Mirkin, Angew. Chem. Int. Ed. **48**, 7787–7791 (2009).
[110] E. Kazuma, N. Sakai, and T. Tatsuma, Chem. Commun. **47**, 5777–5779 (2011).
[111] B. B. Xu, L. Wang, Z. C. Ma, R. Zhang, Q. D. Chen, C. Lv, B. Han, X. Z. Xiao, X. L. Zhang, Y. L. Zhang, K. Ueno, H. Misawa, and H. B. Sun, ACS Nano **8**, 6682–6692 (2014).
[112] M. Gu, H. C. Bao, X. S. Gan, N. Stokes, and J. Z. Wu, Light: Sci. Appl. **3**, e126 (2014).
[113] K. Dholakia and P. Reece, Nano Today **1**, 18–27 (2006).
[114] A. Ashkin, J. M. Dziedzic, J. E. Bjorkholm, and S. Chu, Opt. Lett. **11**, 288 (1986).
[115] T. Čižmár, L. C. D. Romero, K. Dholakia, and D. L. Andrews, J. Phys. B: At. Mol. Opt. Phys. **43**, 102001 (2010).
[116] D. G. Grier, Nature **424**, 810–816 (2003).
[117] M. Daly, M. Sergides, and S. Nic Chormaic, Laser Photonics Rev. **9**, 309–329 (2015).
[118] K. Svoboda and S. M. Block, Opt. Lett. **19**, 930 (1994).
[119] B. B. Xu, R. Zhang, H. Wang, X. Q. Liu, L. Wang, Z. C. Ma, Q. D. Chen, X. Z. Xiao, B. Han, and H. B. Sun, Nanoscale **4**, 6955–6958 (2012).
[120] O. M. Maragò, P. H. Jones, P. G. Gucciardi, G. Volpe, and A. C. Ferrari, Nat. Nanotechnol. **8**, 807–819 (2013).
[121] J. H. G. Huisstede, V. Subramaniam, and M. L. Bennink, Microsc. Res. Techniq. **70**, 26–33 (2007).
[122] J. E. Curtis, B. A. Koss, and D. G. Grier, Opt. Commun. **207**, 169–175 (2002).
[123] S. Mandal, X. Serey, and D. Erickson, Nano Lett. **10**, 99–104 (2010).
[124] E. Jaquay, L. J. Martínez, N. Huang, C. A. Mejia, D. Sarkar, and M. L. Povinelli, Nano Lett. **14**, 5184–5188 (2014).
[125] X. Yang, Y. Liu, R. F. Oulton, X. Yin, and X. Zhang, Nano Lett. **11**, 321–328 (2011).
[126] A. H. Yang, S. D. Moore, B. S. Schmidt, M. Klug, M. Lipson, and D. Erickson, Nature **457**, 71–75 (2009).
[127] T. Shoji and Y. Tsuboi, J. Phys. Chem. Lett. **5**, 2957–2967 (2014).
[128] K. Wang, E. Schonbrun, P. Steinvurzel, and K. B. Crozier, Nat. Commun. **2**, 469 (2011).
[129] A. N. Grigorenko, N. W. Roberts, M. R. Dickinson, and Y. Zhang, Nat. Photonics **2**, 365–370 (2008).
[130] M. L. Juan, M. Righini, and R. Quidant, Nat. Photonics **5**, 349–356 (2011).
[131] Y. Ju, Y. Liao, L. Zhang, Y. Sheng, Q. Zhang, D. Chen, Y. Cheng, Z. Xu, K. Sugioka, and K. Midorikawa, Microfluid. Nanofluid. **11**, 111–117 (2011).
[132] R. An, Y. Li, Y. Dou, H. Yang, and Q. Gong, Opt. Express **13**, 1855–1859 (2005).
[133] Y. Cheng, K. Sugioka, K. Midorikawa, Opt. Lett. **29**, 2007–2009 (2004).
[134] Y. Li, K. Itoh, W. Watanabe, K. Yamada, D. Kuroda, J. Nishii, and Y. Jiang, Opt. Lett. **26**, 1912–1914 (2001).
[135] Y. Kondo, J. Qiu, T. Mitsuyu, K. Hirao, and T. Yoko, Jpn. J. Appl. Phys. **38**, L1146–L1148 (1999).
[136] K. Sugioka, Y. Cheng, and K. Midorikawa, Appl. Phys. A **81**, 1–10 (2005).

[137] R. Drevinskas, M. Gecevicius, M. Beresna, Y. Bellouard, and P. G. Kazansky, Opt. Express **23**, 1428–1437 (2015).
[138] S. LoTurco, R. Osellame, R. Ramponi, and K. C. Vishnubhatla, J. Micromech. Microeng. **23**, 085002 (2013).
[139] K. Chaitanya Vishnubhatla, J. Clark, G. Lanzani, R. Ramponi, R. Osellame, and T. Virgili, Appl. Opt. **48**, G114–118 (2009).
[140] S. Kiyama, S. Matsuo, S. Hashimoto, and Y. Morihira, J. Phys. Chem. C **113**, 11560–11566 (2009).
[141] Y. Bellouard, A. Said, M. Dugan, and P. Bado, Opt. Express **12**, 2120–2129 (2004).
[142] S. Ho, M. Haque, P. R. Herman, and J. S. Aitchison, Opt. Lett. **37**, 1682–1684 (2012).
[143] S. Matsuo, Y. Tabuchi, T. Okada, S. Juodkazis, and H. Misawa, Appl. Phys. A **84**, 99–102 (2006).
[144] V. Maselli, R. Osellame, G. Cerullo, R. Ramponi, P. Laporta, L. Magagnin, and P. L. Cavallotti, Appl. Phys. Lett. **88**, 191107 (2006).
[145] S. Matsuo, H. Sumi, S. Kiyama, T. Tomita, and S. Hashimoto, Appl. Surf. Sci. **255**, 9758–9760 (2009).
[146] F. He, Y. Cheng, Z. Z. Xu, Y. Liao, J. Xu, H. Y. Sun, C. Wang, Z. H. Zhou, K. Sugioka, K. Midorikawa, Y. H. Xu, and X. F. Chen, Opt. Lett. **35**, 282–284 (2010).
[147] Y. Liao, Y. Ju, L. Zhang, F. He, Q. Zhang, Y. Shen, D. Chen, Y. Cheng, Z. Xu, K. Sugioka, and K. Midorikawa, Opt. Lett. **35**, 3225–3227 (2010).
[148] Y. Liao, Y. Shen, L. Qiao, D. Chen, Y. Cheng, K. Sugioka, and K. Midorikawa, Opt. Lett. **38**, 187–189 (2013).
[149] L. E. Criales, P. F. Orozco, A. Medrano, C. A. Rodríguez, and T. Özel, Mater. Manuf. Process. **30**, 890–901 (2015).
[150] S. Darvishi, T. Cubaud, and J. P. Longtin, Opt. Lasers Eng. **50**, 210–214 (2012).
[151] T. N. Kim, K. Campbell, A. Groisman, D. Kleinfeld, and C. B. Schaffer, Appl. Phys. Lett. **86**, 201106 (2005).
[152] L. Amato, Y. Gu, N. Bellini, S. M. Eaton, G. Cerullo, and R. Osellame, Lab Chip **12**, 1135 (2012).
[153] A. Camposeo, M. Polo, A. A. R. Neves, D. Fragouli, L. Persano, S. Molle, A. M. Laera, E. Piscopiello, V. Resta, A. Athanassiou, R. Cingolani, L. Tapfer, and D. Pisignano, J. Mater. Chem. **22**, 9787 (2012).
[154] W. S. Kuo, C. H. Lien, K. C. Cho, C. Y. Chang, C. Y. Lin, L. L. Huang, P. J. Campagnola, C. Y. Dong, and S. J. Chen, Opt. Express **18**, 27550–27559 (2010).
[155] S. Maruo and T. Saeki, Opt. Express **16**, 1174–1179 (2008).
[156] S. Wong, O. Kiowski, M. Kappes, J. K. N. Lindner, N. Mandal, F. C. Peiris, G. A. Ozin, M. Thiel, M. Braun, M. Wegener, and G. von Freymann, Adv. Mater. **20**, 4097–4102 (2008).
[157] S. Ushiba, S. Shoji, K. Masui, P. Kuray, J. Kono, and S. Kawata, Carbon **59**, 283–288 (2013).
[158] H. Xia, J. Wang, Y. Tian, Q. D. Chen, X. B. Du, Y. L. Zhang, Y. He, and H. B. Sun, Adv. Mater. **22**, 3204–3207 (2010).
[159] J. Wang, H. Xia, B. B. Xu, L. G. Niu, D. Wu, Q. D. Chen, and H. B. Sun, Opt. Lett. **34**, 581–583 (2009).
[160] Y. L. Sun, S. M. Sun, B. Y. Zheng, Z. S. Hou, P. Wang, X. L. Zhang, W. F. Dong, L. Zhang, Q. D. Chen, L. M. Tong, and H. B. Sun, IEEE Photonics Technol. Lett. **28**, 629–632 (2016).
[161] B. Kaehr and J. B. Shear, J. Am. Chem. Soc. **129**, 1904–1905 (2007).
[162] Y. L. Sun, W. F. Dong, L. G. Niu, T. Jiang, D. X. Liu, L. Zhang, Y. S. Wang, Q. D. Chen, D. P. Kim, and H. B. Sun, Light: Sci. Appl. **3**, e129 (2014).
[163] J. D. Pitts, P. J. Campagnola, G. A. Epling, and S. L. Goodman, Macromolecules **33**, 1514–1523 (2000).
[164] K. C. Cho, C. H. Lien, C. Y. Lin, C. Y. Chang, L. L. Huang, P. J. Campagnola, C. Y. Dong, and S. J. Chen, Opt. Express **19**, 11732–11739 (2011).
[165] A. Ovsianikov, A. Deiwick, S. Van Vlierberghe, P. Dubruel, L. Moller, G. Drager, and B. Chichkov, Biomacromolecules **12**, 851–858 (2011).
[166] Y. L. Sun, Q. Li, S. M. Sun, J. C. Huang, B. Y. Zheng, Q. D. Chen, Z. Z. Shao, and H. B. Sun, Nat. Commun. **6**, 8612 (2015).
[167] B. P. Chan, J. N. Ma, J. Y. Xu, C. W. Li, J. P. Cheng, and S. H. Cheng, Adv. Funct. Mater. **24**, 277–294 (2014).
[168] Y. L. Sun, D. X. Liu, W. F. Dong, Q. D. Chen, and H. B. Sun, Opt. Lett. **37**, 2973–2975 (2012).
[169] Y. L. Sun, S. M. Sun, P. Wang, W. F. Dong, L. Zhang, B. B. Xu, Q. D. Chen, L. M. Tong, and H. B. Sun, Small **11**, 2869–2876 (2015).
[170] B. Kaehr, N. Ertas, R. Nielson, R. Allen, R. T. Hill, M. Plenert, and J. B. Shear, Anal. Chem. **78**, 3198–3202 (2006).
[171] B. Kaehr, R. Allen, D. J. Javier, J. Currie, and J. B. Shear, P. Natl. Acad. Sci USA **101**, 16104–16108 (2004).
[172] C. F. Lin, C. K. Lin, Y. J. Liu, C. H. Chiang, M. J. Pan, P. P. Baldeck, and C. L. Lin, RSC Adv. **4**, 62882–62887 (2014).
[173] M. Iosin, T. Scheul, C. Nizak, O. Stephan, S. Astilean, and P. Baldeck, Microfluid. Nanofluid. **10**, 685–690 (2010).
[174] C. H. Lien, W. S. Kuo, K. C. Cho, C. Y. Lin, Y. D. Su, L. L. Huang, P. J. Campagnola, C. Y. Dong, and S. J. Chen, Opt. Express **19**, 6260–6268 (2011).
[175] B. B. Xu, R. Zhang, X. Q. Liu, H. Wang, Y. L. Zhang, H. B. Jiang, L. Wang, Z. C. Ma, J. F. Ku, F. S. Xiao, and H. B. Sun, Chem. Commun. **48**, 1680–1682 (2012).
[176] D. M. Eby, N. M. Schaeublin, K. E. Farrington, S. M. Hussain, and G. R. Johnson, ACS Nano **3**, 984–994 (2009).
[177] S. Chernousova, and M. Epple, Angew. Chem. Int. Ed. **52**, 1636–1653 (2013).
[178] S. Zhang, N. Wang, Y. Niu, and C. Sun, Sens. Actuators B **109**, 367–374 (2005).
[179] Y. H. Su, Y. F. Ke, S. L. Cai, and Q. Y. Yao, Light: Sci. Appl. **1**, e14 (2012).
[180] F. G. Chuan, T. Sun, F. Cao, Q. Liu, and Z. Ren, Light: Sci. Appl. **3**, e161 (2014).
[181] J. Liu, Y. Liu, N. Liu, Y. Han, X. Zhang, H. Huang, Y. Lifshitz, S. T. Lee, J. Zhong, and Z. Kang, Science **347**, 970–974 (2015).
[182] K. Ke, E. F. Hasselbrink, Jr., and A. J. Hunt, Anal. Chem. **77**, 5083–5088 (2005).
[183] Y. Liao, J. Song, E. Li, Y. Luo, Y. Shen, D. Chen, Y. Cheng, Z. Xu, K. Sugioka, and K. Midorikawa, Lab Chip **12**, 746–749 (2012).
[184] S. G. Park, S. K. Lee, J. H. Moon, and S. M. Yang, Lab Chip **9**, 3144–3150 (2009).
[185] Y. Tian, Y. L. Zhang, J. F. Ku, Y. He, B. B. Xu, Q. D. Chen, H. Xia, and H. B. Sun, Lab Chip **10**, 2902–2905 (2010).

[186] B. B. Xu, Y. L. Zhang, S. Wei, H. Ding, and H. B. Sun, ChemCatChem **5**, 2091–2099 (2013).
[187] A. Narazaki, Y. Kawaguchi, H. Niino, M. Shojiya, H. Koyo, and K. Tsunetomo, Chem. Mater. **17**, 6651–6655 (2005).
[188] K. Sugioka, Y. Hanada, and K. Midorikawa, Laser Photonics Rev. **4**, 386–400 (2010).
[189] K. Sugioka and Y. Cheng, MRS Bull. **36**, 1020–1027 (2011).
[190] J. Xu, D. Wu, Y. Hanada, C. Chen, S. Wu, Y. Cheng, K. Sugioka, and K. Midorikawa, Lab Chip **13**, 4608–4616 (2013).
[191] J. Xu, D. Wu, J. Y. Ip, K. Midorikawa, and K. Sugioka, RSC Adv. **5**, 24072–24080 (2015).
[192] Y. Hanada, K. Sugioka, H. Kawano, I. S. Ishikawa, A. Miyawaki, and K. Midorikawa, Biomed. Microdevices **10**, 403–410 (2008).
[193] N. Ishikawa, Y. Hanada, I. Ishikawa, K. Sugioka, and K. Midorikawa, Appl. Phys. B **119**, 503–508 (2015).
[194] Y. Hanada, K. Sugioka, I. Shihira-Ishikawa, H. Kawano, A. Miyawaki, and K. Midorikawa, Lab Chip **11**, 2109–2115 (2011).
[195] L. Qiao, F. He, C. Wang, Y. Cheng, K. Sugioka, and K. Midorikawa, Appl. Phys. A **102**, 179–183 (2010).
[196] M. I. Mohammed and M. Desmulliez, Micromachines **5**, 457–471 (2014).
[197] D. Schafer, E. A. Gibson, E. A. Salim, A. E. Palmer, R. Jimenez, and J. Squier, Opt. Express **17**, 6068–6073 (2009).
[198] D. Wu, J. Xu, L. G. Niu, S. Z. Wu, K. Midorikawa, and K. Sugioka, Light: Sci. Appl. **4**, e228 (2015).
[199] D. Wu, L. G. Niu, S. Z. Wu, J. Xu, K. Midorikawa, and K. Sugioka, Lab Chip **15**, 1515–1523 (2015).
[200] C. Lv, H. Xia, W. Guan, Y. L. Sun, Z. N. Tian, T. Jiang, Y. S. Wang, Y. L. Zhang, Q. D. Chen, K. Ariga, Y. D. Yu, and H. B. Sun, Sci. Rep. **6**, 19801 (2016).
[201] J. F. Li, Y. F. Huang, Y. Ding, Z. L. Yang, S. B. Li, X. S. Zhou, F. R. Fan, W. Zhang, Z. Y. Zhou, Y. Wu de, B. Ren, Z. L. Wang, and Z. Q. Tian, Nature **464**, 392–395 (2010).
[202] A. J. Rovner, A. D. Haimovich, S. R. Katz, Z. Li, M. W. Grome, B. M. Gassaway, M. Amiram, J. R. Patel, R. R. Gallagher, J. Rinehart, and F. J. Isaacs, Nature **518**, 89–93 (2015).
[203] Y. Fang, N. H. Seong, and D. D. Dlott, Science **321**, 388–392 (2008).
[204] K. Herman, L. Szabo, L. F. Leopold, V. Chis, and N. Leopold, Anal. Bioanal. Chem. **400**, 815–820 (2011).
[205] B. B. Xu, Z. C. Ma, H. Wang, X. Q. Liu, Y. L. Zhang, X. L. Zhang, R. Zhang, H. B. Jiang, and H. B. Sun, Electrophoresis **32**, 3378–3384 (2011).
[206] H. C. Jeon, C. J. Heo, S. Y. Lee, and S. M. Yang, Adv. Funct. Mater. **22**, 4268–4274 (2012).
[207] H. C. Jeon, C. J. Heo, S. Y. Lee, S. G. Park, and S. M. Yang, J. Mater. Chem. **22**, 4603 (2012).
[208] H. C. Jeon, S. G. Park, S. Cho, and S. M. Yang, J. Mater. Chem. **22**, 23650 (2012).
[209] J. I. Kato, N. Takeyasu, Y. Adachi, H. B. Sun, and S. Kawata, Appl. Phys. Lett. **86**, 044102 (2005).
[210] X. Z. Dong, Z. S. Zhao, and X. M. Duan, Appl. Phys. Lett. **91**, 124103 (2007).
[211] D. Wu, Q. D. Chen, B. B. Xu, J. Jiao, Y. Xu, H. Xia, and H. B. Sun, Appl. Phys. Lett. **95**, 091902 (2009).